REMYELINATION IS ACCELERATED BY EXPERIMENTAL AUTOIMMUNE ENCEPHALOMYELITIS: A NOVEL MODEL FOR THE ELUCIDATION OF IMMUNE-MEDIATED BRAIN REPAIR

by

Anna Claire D. Lamport

Submitted in partial fulfilment of the requirements
for the degree of Master of Science

at

Dalhousie University
Halifax, Nova Scotia
July 2018

Dedicated to my family

TABLE OF CONTENTS

LIST OF TABLES

LIST OF FIGURES

ABSTRACT

Introduction: Experimental autoimmune encephalomyelitis (EAE) and lysophosphatidylcholine (LPC)-induced demyelination are common rodent models of multiple sclerosis (MS). Clozapine and pioglitazone, two drugs used in the treatment of schizophrenia and type 2 diabetes, respectively, were tested in the LPC model to assess their potential to promote remyelination. The EAE and LPC models were then combined to study remyelination in a pro-inflammatory context.

Methods: Female C57BL/6 mice received a bilateral injection of phosphate buffered saline (PBS) and LPC into the corpus callosum, followed by daily oral treatment with clozapine (10 mg/kg) or vehicle, or pioglitazone (15 mg/kg) or vehicle for 7 days. For the dual EAE and LPC model, mice were injected with myelin oligodendrocyte glycoprotein (MOG_{35-55}) or complete Freund's adjuvant (CFA; day 0) and pertussis toxin (PTX; days 0 and 2). LPC and PBS were then injected bilaterally into the corpus callosum on day 7.

Results: Neither clozapine- nor pioglitazone-treated mice exhibited enhanced myelin repair after 7 days relative to vehicle-treated mice. In this dual model, EAE mice exhibited accelerated myelin repair following LPC injection relative to CFA/PTX mice. This was accompanied by increased innate immune cell activation, leukocyte infiltration and pro-inflammatory cytokine gene (IFN-γ, IL-6 and TNF-α) expression in the brain parenchyma of EAE relative to CFA/PTX mice. Immune cell activation that increases the clearance of myelin debris and stimulates oligodendrocyte precursor cell differentiation and survival are proposed to mediate accelerated myelin repair in EAE mice following LPC injection.

Conclusion: This dual model provides a method to identify immune-mediated processes that facilitate remyelination in MS.

LIST OF ABBREVIATIONS AND SYMBOLS USED

ANOVA	Analysis of variance
cDNA	Complementary deoxyribonucleic acid
CFA	Complete Freund's adjuvant
cm	Centimetre
CNS	Central nervous system
CSF	Cerebrospinal fluid
CIS	Clinically isolated syndrome
DMT	Disease-modifying therapy
DPI	Days post-immunization
EAE	Experimental autoimmune encephalomyelitis
EDTA	Ethylenediaminetetraacetic acid
ECNR	Eriochrome cyanine/neutral red
EDSS	Expanded disability status scale
GAPDH	Glyceraldehyde 3-phosphate dehydrogenase
GFAP	Glial fibrillary acidic protein
hr	Hour
Hz	Hertz
Iba1	Ionized calcium binding adapter molecule 1
IFN-γ	Interferon gamma
IL-1β	Interleukin-1beta
IL-4	Interleukin 4
IL-6	Interleukin 6

ip	Intraperitoneal
kg	Kilogram
l	Litre
LPC	Lysophosphatidylcholine
M1	Classically activated macrophages/microglia
M2	Alternatively activated macrophages/microglia
MBP	Myelin basic protein
mg	Milligram
ml	Millilitre
min	Minute
MIP-2	Macrophage inflammatory protein 2
mm	Millimetre
MOG	Myelin oligodendrocyte glycoprotein
MRI	Magnetic resonance imaging
mRNA	Messenger ribonucleic acid
MS	Multiple sclerosis
n	Sample size
ng	Nanogram
O_2	Oxygen
OPC	Oligodendrocyte precursor cell
PBS	Phosphate buffered saline
po	Per os
PPARγ	Peroxisome proliferator-activated receptor gamma

PPMS	Primary progressive multiple sclerosis
PTX	Pertussis toxin
qRT-PCR	Quantitative real-time polymerase chain reaction
RNA	Ribonucleic acid
RRMS	Relapsing-remitting multiple sclerosis
sec	Second
sc	Subcutaneous
SEM	Standard error of the mean
SPMS	Secondary progressive multiple sclerosis
TGF-β	Transforming growth factor beta
TNF-α	Tumor necrosis factor alpha
TNFR1	Tumor necrosis factor receptor 1
TNFR2	Tumor necrosis factor receptor 2
T-PBS	0.5% Triton X-100 in phosphate buffered saline
TZD	Thiazolidinedione
w/v	Weight/volume
β-actin	Beta-actin
μl	Microlitre
μm	Micrometre
μM	Micromolar
%	Percent
°C	Degrees Celsius

ACKNOWLEDGEMENTS

I would first and foremost like to thank my supervisor, Dr. George Robertson. Your knowledge, ideas, encouragement and humour have made the past two years an enjoyable learning experience. I have learned more than I could have imagined and have had a lot of laughs along the way. Elizabeth, there was never a question you didn't have the answer to. There were a lot of things I couldn't have done without your help. Arul and Aurelio, thanks for making the lab a fun place to be. Matthew, lunches won't be the same without you. Thanks for your help with experiments and moral support every day of the last two years. Scott, thanks for lots of laughs along the way. Lauren, thanks for your hard work during the summer. Max, thanks for being someone I can go to for advice. Jordan, I wouldn't be here without you. Thank you for always being confident in me and for being a mentor and a friend I can go to for advice and guidance. You've all been incredibly supportive and I'm grateful to have all of you as friends.

I would like to thank the members of my advisory committee, Dr. Eileen Denovan-Wright and Dr. Denis Dupre, for their guidance and input on my project, and the members of my examining committee, Dr. Eileen Denovan-Wright and Dr. Alexander Easton. Thank you to the entire department of Pharmacology for their ongoing support.

I'd finally like to thank my family. Thank you for your unwavering love and support in everything I do. Having such a supportive and encouraging family has made me confident and passionate about the things I do. Thank you for everything.

CHAPTER 1: INTRODUCTION

1.1 Multiple Sclerosis

Multiple sclerosis (MS) is a neurodegenerative disorder characterized by the autoimmune-mediated destruction of myelin in the central nervous system (CNS), leading to axonal instability and degeneration. Symptoms include muscle weakness, visual impairments, dizziness, incontinence and mood changes (Calabresi, 2004). Individuals are generally diagnosed with MS between the ages of 20 and 49, but symptoms frequently arise years before diagnosis (Gilmour, Ramage-Morin, & Wong, 2018). The precise etiology of the disease remains unknown, but several immunological, genetic and environmental factors have been implicated in the development of MS (Compston & Coles, 2008). At 290 individuals per 100 000 with MS, Canada has one of the highest prevalence rates of MS in the world, with females 2.6 times more likely to be afflicted than men (Gilmour et al., 2018).

MS is classified into 4 common clinical phenotypes: clinically-isolated syndrome (CIS), relapsing-remitting (RRMS), secondary progressive (SPMS) and primary progressive (PPMS). The foundation for a diagnosis of MS is dissemination of lesions in space and time. CIS is defined by the occurrence of the first clinical attack marked by one or more lesions observed on MRI; 60-80% of these patients will go on to develop a clinically definite phenotype of MS (Miller, Chard, & Ciccarelli, 2012). The most common form of the disease affecting 85% of patients, RRMS, is characterized by acute exacerbations of neurological

symptoms (relapses) followed by recovery (Loma & Heyman, 2011). RRMS can evolve into SPMS, in which symptoms worsen gradually without relapses or remission, which eventually occurs in about 80% of those with RRMS (Compston & Coles, 2008). Approximately 10% of MS patients suffer from PPMS, in which a persistent worsening of symptoms begins at the time of disease onset (Dendrou, Fugger, & Friese, 2015).

1.1.1 Pathophysiology of MS

Neurological symptoms in MS arise from inflammatory demyelinating lesions within the CNS. Lesion formation involves the infiltration of myelin-reactive T cells into the CNS through the blood brain barrier, which becomes compromised (Compston & Coles, 2008; Kirk, Plumb, Mirakhur, & McQuaid, 2003). B cells and macrophages are recruited to the lesion site, and the local inflammatory milieu causes activation of microglia and astrocytes (Compston & Coles, 2008). Myelin is phagocytosed by macrophages and microglia, and oligodendrocytes are depleted by the induction of apoptotic cell death (Barnett & Prineas, 2004). Acute demyelination and inflammation impair the conduction of action potentials by axons, with prolonged inflammation resulting in axonal damage and transection (Ferguson, Matyszak, Esiri, & Perry, 1997; Trapp et al., 1998). $CD8^+$ T cells are more numerous than $CD4^+$ T cells within sites of active demyelination and are often concentrated in perivascular regions that surround the lesion border (Gay, Drye, Dick, & Esiri, 1997). Components of complement and immunoglobulins are abundant within the demyelinating area; however, the role of antibodies in

disease pathogenesis is not well understood (Kuhlmann et al., 2017; Storch et al., 1998). Active demyelinating lesions appear histologically as hypercellular with sharp borders (Kuhlmann et al., 2017) and can be detected as gadolinium-enhancing regions by magnetic resonance imaging (MRI), indicating loss of blood brain barrier integrity (Reich, Lucchinetti, & Calabresi, 2018). Autoimmune-mediated demyelination accompanied by persistent inflammation results in axonal transection responsible for sometimes irreversible loss of sensory, motor and cognitive function in MS.

Transition from RRMS to progressive MS is marked by a shift in pathophysiological processes that change the disease state. In chronic lesions, slow and minimal demyelination appears to be secondary to neurodegenerative processes. Although the formation of new active and demyelinating gadolinium-enhancing lesions is rare, a low level of demyelination continues at the borders of existing lesions (Lassmann, Brück, & Lucchinetti, 2007). Despite worsening neurological symptoms, inflammation is sparse within lesions (Frischer et al., 2009). Disease progression measured by the expanded disability status scale (EDSS) is also highly correlated with global atrophy of both the brain and spinal cord (Losseff, Wang, et al., 1996; Losseff, Webb, et al., 1996). These patterns suggest that factors additional to autoimmune-mediated myelin damage drive disease progression in MS.

1.1.2 Remyelination in MS

Remyelination is possible in MS, but eventually fails for reasons that are poorly understood. Following a demyelinating event in the CNS, oligodendrocyte precursor cells (OPCs) proliferate and migrate to the site of the injury where they differentiate into mature, myelin-producing oligodendrocytes (Franklin, 2002; Rawji, Mishra, & Yong, 2016). Experimental models suggest that effective phagocytosis of myelin debris by macrophages and microglia is required before remyelination can occur (Kotter, Li, Zhao, & Franklin, 2006). Myelin produced by new oligodendrocytes following demyelination is thinner relative to healthy axons that have not undergone demyelination, but is typically sufficient to restore conduction and confer protection to the axon (Franklin & Ffrench-Constant, 2008). Remyelination is frequently observed at early stages of the disease (Goldschmidt, Antel, König, Brück, & Kuhlmann, 2009), but after repeated cycles of demyelination, remyelination ultimately fails in most patients (Franklin, 2002). The development of remyelinating agents is therefore a major therapeutic goal in MS research.

1.1.3 Treatment of MS

There is no cure for MS, but 14 Health Canada approved disease-modifying therapies (DMTs) are available for treatment of the disease, as outlined in Table 1. Current treatments target the peripheral immune cell populations responsible for CNS damage. They act in a variety of ways, which include reducing lymphocyte infiltration into the CNS, suppressing circulating lymphocyte numbers

Table 1. Disease-modifying therapies approved by Health Canada for the treatment of MS.

Generic Name (Brand Names)	Drug Class	Mechanism of Action
Alemtuzumab (Lemtrada)	Monoclonal antibody against CD52	Depletes mature lymphocytes
Cladribine (Mavenclad)	Antimetabolite	Depletes T and B lymphocytes
Dimethyl fumarate (Tecfidera)	Activator of Nrf2 pathway	Mechanism of action unknown
Fingolimod (Gilenya)	Sphingosine 1-phosphate receptor modulator	Prevents lymphocyte egress from lymph nodes
Glatiramer acetate (Copaxone, Glatect)	Mixture of 4 synthetic amino acids	Mechanism of action unknown, but may compete with myelin for antigen presentation
Interferon beta-1a (Avonex, Rebif)	Cytokine	Reduces pro-inflammatory cytokine production and enhances anti-inflammatory cytokine production
Interferon beta-1b (Betaseron, Extavia)	Cytokine	Reduces pro-inflammatory cytokine production and enhances anti-inflammatory cytokine production
Natalizumab (Tysabri)	Monoclonal antibody against α4 integrin	Prevents leukocyte migration across the blood brain barrier
Ocrelizumab (Ocrevus)	Monoclonal antibody against CD20	Depletes B cells
Peginterferon beta-1a (Plegridy)	Cytokine (Pegylated interferon beta-1a)	Reduces pro-inflammatory cytokine production and enhances the generation of anti-inflammatory cytokines
Teriflunomide (Aubagio)	Dihydroorotate dehydrogenase inhibitor	Blocks lymphocyte proliferation through inhibiting *de novo* pyrimidine synthesis

through sequestration or depletion and decreasing pro-inflammatory cytokine production (Baecher-Allan, Kaskow, & Weiner, 2018). Most DMTs are only approved for the treatment of RRMS and those with SPMS that still experience relapses. However, Ocrelizumab, an anti-B cell therapy, has recently been shown to be modestly effective in the treatment of PPMS (Montalban et al., 2017), becoming the first DMT approved for PPMS. No DMTs are capable of neural cell protection, myelin repair or preventing axonal loss following inflammatory damage, highlighting a void in treatment options.

1.2 Experimental Autoimmune Encephalomyelitis

Experimental autoimmune encephalomyelitis (EAE) is the most common model used to study MS disease processes and to predict the efficacy of therapeutics in the treatment of MS (Handel, Lincoln, & Ramagopalan, 2011). Induction of EAE involves immunization with a myelin antigen emulsified in an immune adjuvant. The EAE model can be highly variable in pathology and disease course depending on both the myelin antigen used (myelin basic protein, myelin oligodendrocyte glycoprotein, proteolipid protein) and study species (mice, rats, non-human primates; Gold, Linington, & Lassmann, 2006). Immunization of C57BL/6 mice with myelin oligodendrocyte glycoprotein amino acids 35-55 (MOG_{35-55}) emulsified in complete Freund's adjuvant (CFA) produces a monophasic disease course (Bittner, Afzali, Wiendl, & Meuth, 2014), making it useful for studying an acute relapse. Pertussis toxin (PTX), administered both at the time of immunization and two days later, is required for disease induction and

is thought to act by increasing permeability of the blood brain barrier (Bittner et al., 2014). Beginning 9-12 days following MOG_{35-55} immunization, mice develop ascending hindlimb paralysis (originating at the tail) followed by gradual recovery, with retention of minor motor impairment for at least a year following induction (Jones et al., 2008). Infiltrating immune cells, largely $CD4^+$ T cells and macrophages, produce demyelination in the spinal cord and cerebellum, with minimal involvement of the forebrain (Constantinescu, Farooqi, O'Brien, & Gran, 2011; Höflich et al., 2016). Demyelinated areas in the spinal cord are associated with axonal loss; this continues after clinical symptoms have plateaued, ultimately yielding a 50% reduction in the number of axons in cervical and lumbar regions of the spinal cord (Jones et al., 2008). These autoimmune and pathophysiological features and resultant motor impairments that resemble MS have led to the wide-spread use of this model.

1.2.1 EAE has been instrumental in the development of MS therapeutics

EAE has been integral in the development and approval of 6 DMTs currently approved for the treatment of MS (Gold et al., 2006). However, EAE experimentation has also led to the testing of therapeutics in MS clinical trials that were unsuccessful, most notably the anti-tumor necrosis factor (TNF) drug Lenercept. Lenercept, a TNF fusion protein, was able to reduce EAE disease severity in mice, but caused an increase in the frequency of relapses when tested in people with MS (The Lenercept Multiple Sclerosis Study Group, 1999). EAE thus has significant limitations as a reliable model for predicting the clinical

efficacy of putative MS therapeutics. Like MS, EAE involves auto-reactive T cells that orchestrate demyelination of the CNS. However, $CD4^+$ T cells predominate in EAE (Gold et al., 2006), while it is well established that $CD8^+$ T cells drive MS. In MS, $CD8^+$ cells are more numerous and show evidence of clonal expansion, while the less numerous $CD4^+$ cells detected in this disease do not (Sriram & Steiner, 2005). Demyelination in EAE is only observed in white matter tracts of the spinal cord, cerebellum, hindbrain and optic nerve of mice (Constantinescu et al., 2011), whereas pathological abnormalities can be observed throughout the CNS of people with MS, including the forebrain white and gray matter as well as the optic nerve, brain stem and spinal cord (Compston & Coles, 2008). Additionally, demyelination observed in EAE is diffuse and sporadic compared to other models, making it difficult to study neuroprotection and remyelination. EAE has proven useful in the establishment of DMTs that target inflammation, but in the search for therapeutics that promote protection or repair, EAE is not the ideal model candidate.

1.3 Lysophosphatidylcholine-Mediated Demyelination

Lysophosphatidylcholine (LPC) comprises approximately 8% of the phospholipids present in the white matter of the human brain (Papadopoulos, Cevallos, & Hess, 1960). Stereotaxic injection of concentrated LPC into white matter tracts of the rodent CNS leads to rapid focal demyelination that can be detected within 30 minutes (Hall, 1972). LPC is inserted into the myelin membrane and disrupts the myelin lamellae by forming lipid-protein-LPC aggregates, ultimately leading to

oligodendrocyte death (Gregson, 1989; Plemel et al., 2018). Exogenous LPC is metabolized fully by 24 hours following injection through acylation that converts LPC into phosphatidylcholine (Plemel et al., 2018; Webster & Alpern, 1964). Demyelination mediated by LPC peaks between 24 and 72 hours and remyelination begins 7 days post-injection, with near-complete remyelination occurring after 3 weeks in the mouse spinal cord (Jeffery & Blakemore, 1995; Keough, Jensen, & Yong, 2015). LPC primarily causes lysis of myelin membranes, sparing underlying axons (Keough et al., 2015). Demyelination by LPC leaves axons susceptible to damage and impaired axonal transport, which is also observed in MS lesions, but it has been shown that these axons are remyelinated (Höflich et al., 2016; Schultz et al., 2017).

1.3.1 Immune involvement in the LPC model

While the primary effect of LPC injection is myelin loss, it also induces a variety of immunological events. Following LPC injection into the mouse spinal cord, permeability of the blood brain barrier and expression of blood vessel adhesion molecules are elevated both near and distal to the site of injection (Ousman & David, 2000). $CD4^+$ and $CD8^+$ T cells are observed throughout the lesion 6 hours after LPC injection; the presence of these cells is required for maximal LPC-mediated demyelination and subsequent macrophage recruitment and activation (Ghasemlou, Jeong, Lacroix, & David, 2007; Ousman & David, 2000). Macrophages are numerous within demyelinating lesions (Keough et al., 2015) and play integral roles in lesion development and repair, including early

phagocytosis of myelin debris and facilitation of OPC differentiation (Kotter, Setzu, Sim, Van Rooijen, & Franklin, 2001; Miron et al., 2013; Ousman & David, 2000). Injection of LPC involves mechanical disruption of the blood barrier, but stereotaxic injection of PBS alone into the corpus callosum produces only minor immune activation that is limited to the immediate vicinity of the needle path (Tejedor et al., 2017). Therefore, in addition to demyelination, LPC triggers an immune response, albeit minor relative to EAE, that is not attributable to the mechanical disruption of the blood brain barrier.

1.4 Potential Remyelinating Candidates for MS

1.4.1 Clozapine in the treatment of schizophrenia

Schizophrenia is a disorder characterized by positive symptoms (psychosis, delusions and visual/auditory hallucinations) and negative symptoms (deficits in emotions and social interaction), in addition to cognitive impairments (Owen, Sawa, & Mortensen, 2016; Patel, Cherian, Gohil, & Atkinson, 2014). These deficits likely arise from abnormalities in dopamine, serotonin and glutamate signalling in the CNS (Patel et al., 2014). Schizophrenia is also characterized by myelin atrophy and reduced oligodendrocyte activity (Ardekani, Nierenberg, Hoptman, Javitt, & Lim, 2003; Flynn et al., 2003; Hakak et al., 2001). Clozapine is an atypical antipsychotic that acts primarily as an antagonist at serotonin 5-HT2A and dopamine D2 receptors (Seeman, 2014). Clozapine is highly effective at improving positive and negative symptoms, suicidal ideation and aggressive behaviour in people with schizophrenia (Naheed & Green, 2001). However,

clozapine treatment is associated with several side effects, namely agranulocytosis, weight gain and bowel obstruction (Alvir, Lieberman, Safferman, Schwimmer, & Schaaf, 1993; Seeman, 2014). Therefore, clozapine is only indicated for patients with schizophrenia that are resistant to other antipsychotic drugs and remains the most effective treatment option for this patient population (Kane, Honigfeld, Singer, & Meltzer, 1988; Stroup, Gerhard, Crystal, Huang, & Olfson, 2016).

1.4.2 Evidence for the capacity of clozapine to promote remyelination

Due to the involvement of myelin pathology in schizophrenia and the efficacy of clozapine in treatment-resistant schizophrenia, there has been recent interest in investigating clozapine as a treatment for MS. Remyelination requires the proliferation and recruitment of OPCs to the lesion site and maturation into oligodendrocytes, both of which are processes that likely become impaired in MS (Franklin, 2002). When treated with clozapine, cultured rat oligodendrocytes show increased glycolytic activity and enhanced production of galactocerebroside, a lipid component of myelin (Steiner et al., 2014). Cuprizone is a copper chelator that prevents the differentiation of OPCs into mature oligodendrocytes *in vitro,* and when administered orally to rodents *in vivo* selectively depletes mature oligodendrocytes, causing demyelination in the CNS (Cammer, 1999). Clozapine treatment overcomes the inhibitory effects of cuprizone on OPC differentiation, resulting in increased numbers of mature oligodendrocytes (Xu, Yang, & Li, 2014). Clozapine also reverses cuprizone-

induced demyelination in mice, enabling enhanced production of myelin basic protein and improved behavioural outcomes (Xu, Yang, Mcconomy, Browning, & Li, 2010). This atypical antipsychotic has also be shown to reduce EAE disease severity when administered orally beginning both at the time of EAE induction (prophylactically) or just before disease onset (Green et al., 2017; O'Sullivan et al., 2014). Clozapine's success in rodent models of MS and its beneficial effects on oligodendrocytes make it a promising candidate as a remyelinating therapy in MS.

1.4.3 Pioglitazone in the treatment of type 2 diabetes

Type 2 diabetes is a metabolic disorder characterized by a dysregulated feedback loop involving glucose homeostasis. Progressive resistance to insulin in normally insulin-sensitive tissue (liver, skeletal muscle and adipose tissue) leads to a compensatory increase in insulin production by β-cells in the pancreas, followed by an eventual reduction in the function and number of β-cells (Kahn, Cooper, & Del Prato, 2015). Pioglitazone, a member of the thiazolidinediones (TZDs) drug class, is a peroxisome proliferator-activated receptor gamma (PPARγ) agonist. Pioglitazone treatment normalizes blood glucose levels by increasing insulin sensitivity in liver, skeletal muscle and adipose tissue by the induction of peroxisome proliferator-activated receptor-driven genes involved in the insulin response (Meriden, 2004). When compared to metformin, a first-line type 2 diabetes therapeutic, pioglitazone leads to similar improvements in several metabolic parameters indicative of enhanced insulin sensitivity (Schernthaner,

Matthews, Charbonnel, Hanefeld, & Brunetti, 2004). However, pioglitazone treatment is associated with weight gain, edema and an increased risk of heart failure (Liao et al., 2017) and is therefore indicated for patients with normal cardiovascular function that do not respond to first-line therapies.

1.4.4 Evidence for the disease-modifying effects of pioglitazone in MS

Studies conducted in pre-clinical models and preliminary MS clinical trials suggest that pioglitazone may be a candidate for the treatment of MS. Treatment with pioglitazone has been shown to reduce the production of pro-inflammatory cytokines by cultured rodent microglia and astrocytes following activation (Storer, Xu, Chavis, & Drew, 2005) and to promote the differentiation of cultured OPCs to mature oligodendrocytes (Bernardo, Bianchi, Magnaghi, & Minghetti, 2009; De Nuccio et al., 2011). Additionally, pioglitazone treatment was associated with a reduction in the capacity of myelin-reactive $CD4^+$ T cells to migrate across a compromised endothelial cell barrier in culture conditions (Klotz et al., 2007). When tested in both a monophasic and relapsing model of EAE in rats, oral pioglitazone administration was effective at reducing disease severity that was associated with reduced demyelination and leukocyte infiltration into the CNS (Feinstein et al., 2002). These animal studies suggest pioglitazone may be capable of reducing pro-inflammatory cytokine production, reducing leukocyte infiltration and/or promoting remyelination in MS.

When isolated from the peripheral blood of people with MS, autoreactive T cells showed decreased production of pro-inflammatory cytokines and a reduced proliferative capacity following treatment with pioglitazone (Schmidt et al., 2004). Monocytes isolated from people with MS are less effective at myelin phagocytosis compared to those isolated from healthy controls, but pioglitazone was able to normalize myelin phagocytosis and induce a shift toward an M2-polarized (anti-inflammatory) phenotype (Natrajan et al., 2015). Pioglitazone was also tested in several small cohorts of people with MS. These studies reported improvement in disease outcomes and MRI measures of lesion burden following oral treatment with pioglitazone (Kaiser et al., 2009; Pershadsingh et al., 2004; Schernthaner et al., 2004). These encouraging findings have fueled intense interest in repositioning pioglitazone for MS and stimulated basic research concerning the mechanism by which this drug improves remyelination in animal models of autoimmune-mediated and toxin-induced demyelination.

1.5 Rationale

No therapeutics are approved for the treatment of MS that directly promote myelin repair and protect from axonal loss following an inflammatory attack. Treatment options for progressive MS, where disease processes are dominated by neurodegeneration and demyelination, are very limited. Clozapine and pioglitazone have demonstrated the potential to promote recovery in animal models of MS. However, it is not known whether these effects are primarily immunomodulatory in nature or mediated by the induction of remyelination.

1.6 Research Objectives

1.6.1 Comparison of remyelination by clozapine and pioglitazone following LPC-induced focal demyelination in the corpus callosum

The first objective of this study was therefore to assess the potential for clozapine and pioglitazone to promote remyelination in the LPC model of focal demyelination, a model in which these drugs have not been tested before. It is hypothesized that:

i) Both clozapine and pioglitazone will enhance remyelination following LPC-mediated demyelination in the corpus callosum.

1.6.2 Combining the EAE and LPC models to better reflect the conditions responsible for demyelination and repair in MS

A failure to identify neuroprotective and reparative therapies may be due to a lack of appropriate models for drug screening. Limitations in the EAE and LPC models necessitate the use of multiple models to encompass the complex conditions observed in MS. Additionally, predictions from these models have sometimes proven to be inaccurate for people with MS. EAE mimics hallmark features of MS such as autoimmune-mediated demyelination, inflammation, axonal damage and motor impairments. However, regions of demyelination are sporadic and inconsistent in location, making it difficult to study reparative processes. LPC-mediated demyelination produces focal myelin loss in a highly reproducible manner with sparing of underlying axons, allowing for the study of remyelination processes in relative isolation from neurodegeneration. However, the

inflammatory environment characteristic of MS is incomplete, making direct translation to a clinical context uncertain. The LPC and EAE models were therefore combined to overcome limitations specific to each of these models and thus create a novel model that better recapitulates disease processes observed in MS. Consequently, the second objective of this study was to characterize the effects of LPC injection in the corpus callosum of mice with EAE. It is hypothesized that:

i) Pro-inflammatory cell populations already primed for the destruction of myelin in EAE mice will enhance the extent of demyelination mediated by LPC injection relative to mice that were not previously exposed to the myelin antigen.

ii) LPC lesions in EAE mice will exhibit impaired remyelination due to the increased presence of infiltrating leukocytes and activation of resident glial cells.

CHAPTER 2: METHODS

2.1 Animal Care

All animal experiments were approved by the University Committee on Laboratory Animals at Dalhousie University and conducted in accordance with Canadian Council on Animal Care standards.

2.2 Lysophosphatidylcholine (LPC) Model

2.2.1 Lysophosphatidylcholine (LPC) surgery

Female C57BL/6 mice (n = 34) between the ages of 10 and 12 weeks (Charles River) were anesthetized with isoflurane (2.5%, O_2 1 l/min) and placed in the stereotactic frame. A lubricant was placed on the eyes and the head shaved. The skin overlaying the skull was disinfected with isopropyl alcohol and betadine and a vertical incision made 1 cm in length to expose the skull. Two bilateral holes were made in the skull 1.0 mm rostral and 1.0 mm lateral to bregma using a fine drill. An injection of LPC (1 μl of 1% in PBS; Sigma-Aldrich, catalog # L4129) was made into the right corpus callosum and 1 μl of phosphate buffered saline (PBS) into the left corpus callosum. Both injections were 2.3 mm ventral to the surface of the skull, and made using a 7000 series 2 μl Neuros syringe (Hamilton, catalog # 65459-01). The needle was left in place for 3 min following injection to prevent backflow. The needle was then slowly retracted and the incision sutured. Mice received a subcutaneous (sc) injection of ketoprofen (5 mg/kg) for analgesia and monitored closely following surgery to ensure proper recovery from anesthesia.

2.2.2 LPC storage and preparation

LPC was diluted in PBS at 1% w/v and sonicated for 15 min before being aliquoted. LPC aliquots were stored in 150 μl volumes at -80°C. On the day of surgery, one LPC aliquot was thawed and sonicated for 30 min at 40 Hz.

2.2.3 Treatment with vehicle or clozapine

Beginning 24 hours (hr) after surgery, two groups of mice were orally gavaged (po) with either vehicle (distilled water, 100 μl; n = 8) or clozapine (10 mg/kg; n = 8) once daily for 7 days.

2.2.4 Treatment with vehicle or pioglitazone

Beginning 24 hr following surgery, two groups of mice received either vehicle (NEOBEE, 100 μl, po; n = 9) or pioglitazone (15 mg/kg, po; n = 9) once daily for 7 days.

2.3 Dual EAE and LPC Model

2.3.1 EAE induction

Two groups of female C57BL/6 mice between the ages of 10 and 12 weeks, each composed of 32 animals, were anesthetized with isoflurane. The EAE group received bilateral injections (100 μl/injection, sc) at the base of the tail of myelin oligodendrocyte glycoprotein amino acids 35-55 (MOG_{35-55}, GenScript, amino acid sequence: MEVGWYRSPFSRVVHLYRNGK; 150 μg in 100 μl) emulsified in complete Freund's adjuvant (CFA) containing desiccated *Mycobacterium*

tuberculosis (5 mg/ml, BD Pharmingen). The CFA/PTX group was injected in the same fashion with CFA emulsified in PBS (100 μl/injection, sc). All mice were then injected intraperitoneally (ip) with pertussis toxin (300 ng in 200 μl of PBS, Sigma-Aldrich). Two days later, all mice received a second injection of pertussis toxin (300 ng, ip; Figure 1).

2.3.2 Stereotaxic surgery

Seven days later, the CFA/PTX and EAE groups received injections of PBS and LPC into the corpus callosum of the left and right hemisphere, respectively, as described in section 2.2.1. Three CFA/PTX mice were excluded from analysis due to inadequate injection of LPC.

2.3.3 Clinical Scoring

Starting 7 days post-immunization (DPI), all mice were weighed daily and assigned a clinical score to assess motor deficits: 0, no motor deficits; 0.5, hooked tail; 1.0, bilateral hindlimb splay and hooked tail; 1.5, fully flaccid tail; 2.0, minor walking deficits; 2.5, major walking deficits; 3.0, dropped pelvis; 3.5, unilateral hindlimb paralysis; 4.0, bilateral hindlimb paralysis; 4.5, forelimb paralysis; and 5.0, moribund.

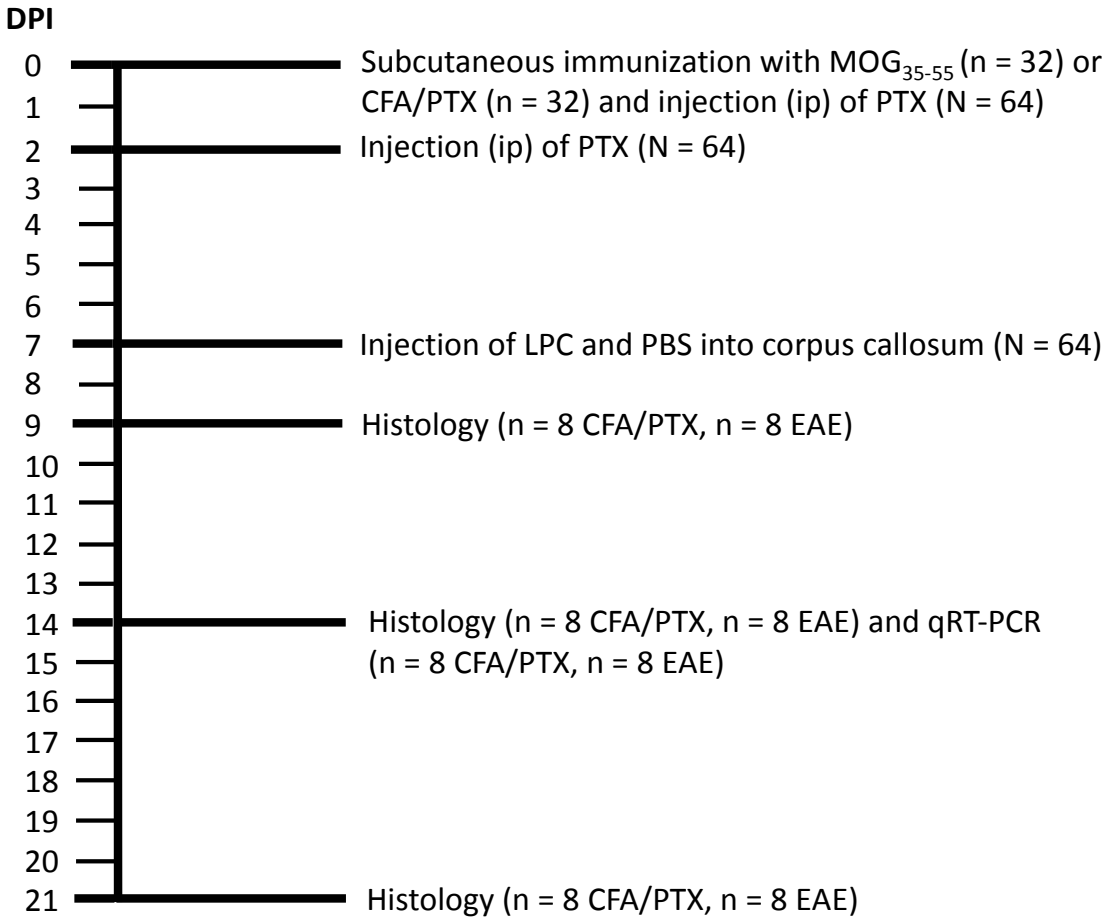

Figure 1. Timeline of procedures, treatments and sample sizes in the dual EAE and LPC model. DPI = days post-immunization, MOG_{35-55} = myelin oligodendrocyte glycoprotein amino acids 35-55, CFA = complete Freund's adjuvant, ip = intraperitoneal, PTX = pertussis toxin, PBS = phosphate buffered saline.

2.4 Tissue Collection, Processing and Sectioning for Histology

At the time of sacrifice, mice were administered a lethal dose of sodium pentobarbital (150 mg/kg, ip). Once at surgical plane, mice were transcardially perfused with 10 ml of PBS followed by 10 ml of 4% paraformaldehyde. Brains were removed and allowed to post-fix in 4% paraformaldehyde for 48 hr. Each brain was then placed in 15% sucrose dissolved in PBS and transferred to 30% sucrose dissolved in PBS once it had sunk. Once the brain had sunk in 30% sucrose, 20 μm thick coronal sections were cut using a cryostat that spanned the PBS and LPC injection sites, placed on SuperFrost slides and stored at -20°C**.**

2.5 Eriochrome Cyanine and Neutral Red Staining

Every second section from each brain sample was stained with eriochrome cyanine (Honeywell Fluka) and counterstained with neutral red (Acros Organics) according to the following procedure. Slides were removed from the freezer and allowed to thaw. Once at room temperature, sections were immersed in a descending series of ethanol concentrations for 3 min each: 100%, 100%, 95%, 95%, 70% and 70%. Sections were then rinsed in a bath of tap water and placed in eriochrome cyanine staining solution (0.16% eriochrome cyanine, 0.4% H_2SO_4, 0.4% $FeCl_3$ in distilled water) for 15 min followed by tap water for 1 min. Sections were then dipped in 0.5% ammonium hydroxide 5-7 times to remove non-specific staining and again placed in tap water for 1 min. Sections were next placed in neutral red stain (1% in distilled water) for 2 min followed by 1 min in tap water. Lastly, the slides were dehydrated through immersion in an ascending series of

ethanol concentrations: 70%, 70%, 95%, 95%, 100% and 100%, followed by placement in xylene to remove all water and cover-slipped with CytoSeal mounting medium. Sections were imaged at 100X magnification using a Zeiss Axioplan II microscope.

2.6 Immunohistochemistry

Brain sections were allowed to reach room temperature. The edges of the slides were traced with an ImmEdge Hydrophobic Barrier PAP pen (Vector Laboratories) and the sections rehydrated with 0.5% Trition X-100 in PBS (T-PBS). For detection of activated macrophages/microglia, sections were stained with antisera raised again Iba1. For detection of leukocytes, sections were stained with antisera raised again CD45. For detection of oligodendrocyte precursor cells, sections were stained with antisera raised against NG2.

Sections stained for NG2 were first counterstained with FluoroMyelin Red (1:100, ThermoFisher, catalog # F34652) for 20 min, followed by three 3-min washes with T-PBS. For Iba1 and CD45 staining, sections were blocked with 10% Goat serum and 10% Donkey serum in T-PBS for 1 hr at room temperature. For NG2 staining, sections were blocked with 20% normal Goat serum for 1 hr at room temperature. Sections were then incubated with the primary antibodies diluted in T-PBS for 18 hr at 4 °C. The following primary antibodies were used: Rabbit anti-Iba1 (1:500, Wako Pure Chemical Industries, Code No. 019-19741), Rat anti-CD45 (1:12, BD Pharmingen, catalog # 550539) and Rabbit anti-NG2 (1:200,

Chemicon, AB5320). The next day, sections were washed for three 3-min washes in T-PBS and incubated with the secondary antibodies diluted in T-PBS. The following secondary antibodies were used: Goat anti-Rabbit IgG AlexaFluor 488 (1:500 for Iba1, 1:250 for NG2; ThermoFisher, catalog # A-11008) and Donkey anti-Rat IgG AlexaFluor 594 (1:500, ThermoFisher, catalog # A-21209). Sections were then washed for three 3-min washes in T-PBS and cover-slipped using Fluoromount mounting medium. Slides were sealed with nail polish and imaged at 100X magnification using the Zeiss AxioImager Z2.

2.7 LPC Lesion Volume Estimation

Using Fiji (ImageJ) software, the cross-sectional area of demyelination on every section stained with eriochrome cyanine was measured by tracing the border of demyelination within the corpus callosum. The cross-sectional area of demyelination was multiplied by 20 μm to account for section thickness and these values plotted to calculate area under the curve as a measure of volume using Prism 7 software.

2.8 Quantification of Corpus Callosum White Matter Loss in the Dual EAE and LPC Model

Every second slide extending from 0.4 mm rostral to 1.2 mm caudal of the needle tract was stained with eriochrome cyanine and assessed for white matter loss within the corpus callosum. The rostral-caudal limits of quantification were determined by the largest LPC lesion in CFA mice at 7 days following LPC injection (DPI 14). Injection of LPC into the corpus callosum of naïve mice

produced a discrete region of demyelination with borders that could be easily discerned and thus traced. By contrast, LPC injection into the corpus callosum of EAE mice often resulted in multiple regions of diffuse white matter loss making it difficult to accurately trace the borders of these lesions (Figure 2A). To overcome this problem, a modified version of the Cavalieri method of volume estimation was used. Using Fiji (ImageJ) software, a grid of crosses, each associated with an area of 500 μm^2, was placed over the image and the number of crosses overlaying a region of white matter loss was counted and recorded (Figure 2B). A region of white matter loss was classified as absence of myelin (blue) staining and was only counted if it spanned two adjacent crosses. The number of crosses multiplied by 500 μm^2 produced the cross-sectional area of white matter loss. The cross-sectional area was multiplied by 20 μm to account for section thickness, and these values were used to plot lesion size (Y axis) against distance from the injection site (X axis) for each lesion. The area under each of these curves was calculated to obtain the volume of white matter loss using Prism 7 software.

2.9 Validation of the Modified Version of the Cavalieri Method

To determine the optimal cross size for measuring white matter loss, LPC lesions in three randomly selected CFA mice were estimated using crosses with an associated area of 2000, 1000 or 500 μm^2. The resultant volume estimations

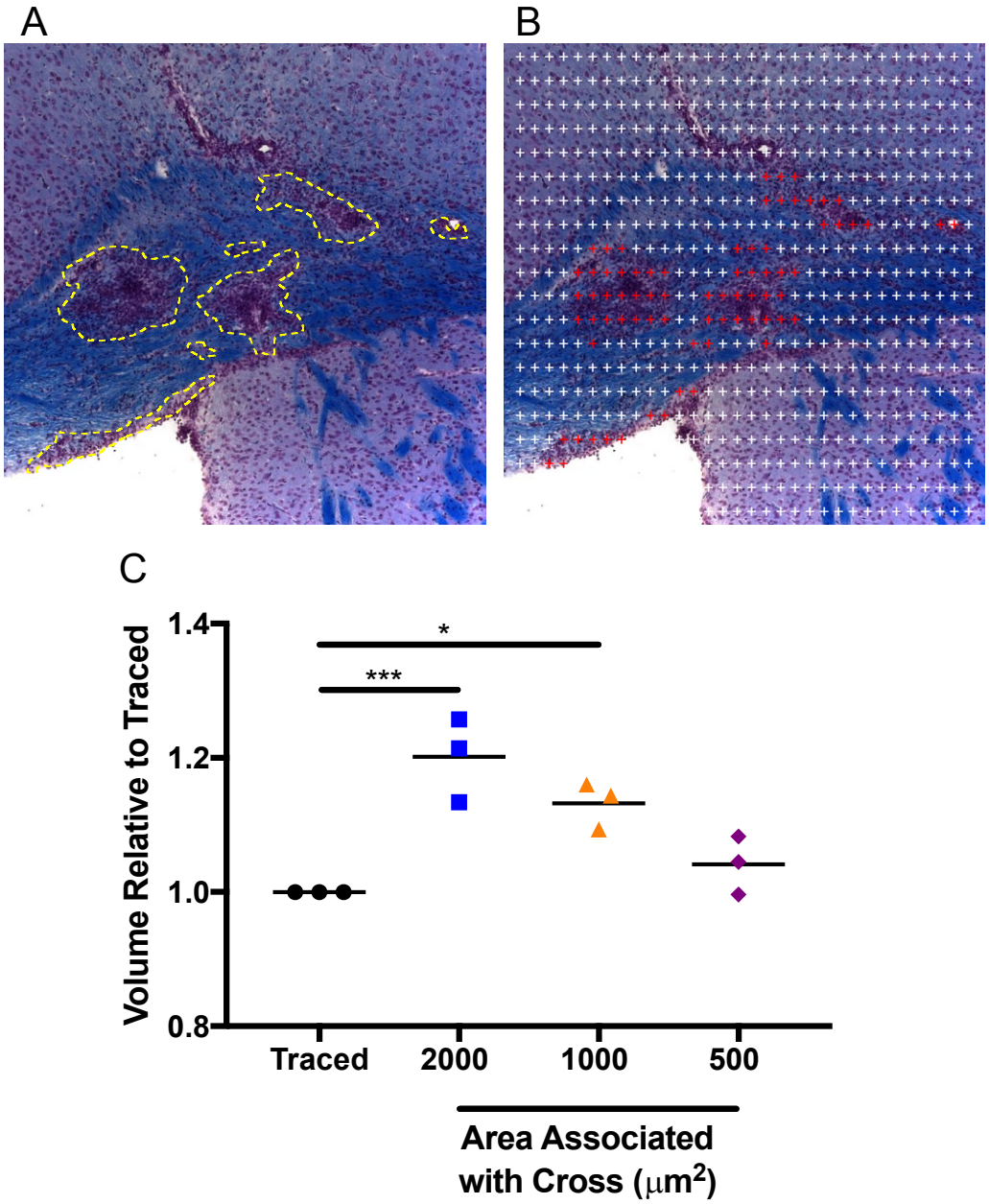
A
B
C
Volume Relative to Traced
1.4
1.2
1.0
0.8
*
***
Traced
2000
1000
500
Area Associated
with Cross (μm²)

Figure 2. The modified Cavalieri method of volume estimation. (A) Representative eriochrome cyanine/neutral red-stained tissue section showing the LPC lesion in an EAE mouse. (B) A grid of crosses was overlaid on this image to estimate white matter loss. The number of crosses (red) that contacted a region devoid of eriochrome cyanine staining was counted and multiplied by the area associated with each cross to determine the cross-sectional area of white matter loss on each section. Grid is representative. (C) Comparison of white matter loss volume estimations using the tracing method and the modified Cavalieri method with crosses of varying size (2000, 1000 or 500 μm^2). The volume of white matter loss was estimated using a grid with crosses 2000, 1000, or 500 μm^2 in size. The resultant vales were normalized to the traced volume, which was defined as a value of 1. When using crosses with an associated area of 2000 or 1000 μm^2, the estimated volume was larger than the traced volume. Using crosses 500 μm^2 in size, the estimated volume was similar to that calculated by tracing. Data represent the mean $\pm$ SEM. *$p < 0.05$, ***$p < 0.001$, one-way ANOVA followed by Tukey's post-hoc analysis.

were converted to a fraction of the traced volume, defined as equaling 1. A cross size corresponding to an area of 500 μm^2 yielded a similar volume as that obtained by traced volume estimation (Figure 2C). A grid with crosses, each 500 μm^2 in size, was therefore used to estimate the volume of white matter loss in the corpus callosum.

2.10 Fluorescence Quantification

The average fluorescent intensity of Iba1, CD45 and NG2 immunoreactivities was measured as the mean gray value using Fiji (ImageJ) software. The lesion area used for quantification of Iba1, CD45 and NG2 immunoreactivities was defined by tracing the zone of white matter loss in an adjacent section stained with eriochrome cyanine or Fluoromyelin.

2.11 Quantitative RT-PCR (qRT-PCR)

Following transcardial perfusion with 10 ml of PBS, the brain was removed and placed in a brain block on ice. Brain tissues were dissected from coronal sections spanning 1 mm rostral and 2 mm caudal to the injection sites using a razor blade. A transverse cut was made connecting the most ventral tips of the corpus callosum to remove the ventral portion of the brain and a sagittal cut made to separate the hemispheres. Brain samples were then placed immediately into a tube containing PureZol and zirconium beads. Next, samples were homogenized for 40 seconds (sec) using a BeadBug microtube homogenizer. Total RNA was then extracted using the Aurum Total RNA Fatty and Fibrous Tissue Kit (Bio-Rad,

catalog # 7326830) according the manufacturer's guidelines. A Bio-Rad Experion bioanalyzer with an RNA StdSense analysis kit (Bio-Rad) was used to determine the quality and purity of the RNA samples. Experion analysis revealed that all of the samples were of acceptable quality and purity (above 7.5). RNA quantity was then measured by duplicate determinations using an Epoch microplate spectrophotometer (BioTek Instruments) and the samples stored at -80°C. Synthesis of complementary DNA (cDNA) through reverse transcription was performed with the iScript cDNA synthesis kit (Bio-Rad, catalog # 1708890) using 1 μg of RNA from each sample. Quantitative RT-PCR (qRT-PCR) was performed according to MIQE guidelines (Bustin et al., 2009) using the SsoFast EvaGreen Supermix kit (Bio-Rad, catalog # 172-5203). Primers were obtained from Invitrogen and diluted in Tris-EDTA, pH = 8. Samples were analyzed in triplicate with the BioRad C1000 Touch Thermal Cycler (96 well) according to the following cycling parameters: 95°C x 3 min + (95°C x 10 sec + 60°C x 10 sec + plate reading) x 40 cycles. Analysis of relative mRNA levels was performed using the ΔΔCq method with Bio-Rad Maestro software, using GAPDH and β-actin as reference genes. Primer sequences of the genes assessed are presented in Table 2.

2.12 Statistical Analyses

All data sets were analyzed using a one-way ANOVA with Tukey's post-hoc test.

Table 2. Forward and reverse primer sequences used for qRT-PCR. Primers were obtained from Invitrogen as a lyophilized powder and reconstituted with Tris-EDTA (pH = 8) to a concentration of 40 μM.

Gene name	Forward nucleotide sequence	Reverse nucleotide sequence
IFN-γ	ATGAACGCTACACACTGCATC	CCATCCTTTTGCCAGTTCCTC
TNF-α	CAGGCGGTGCCTATGTCTC	CGATCACCCCGAAGTTCAGTAG
IL-6	CTGCAAGAGACTTCCATCCAG	AGTGGTATAGACAGGTCTGTTGG
IL-1β	GAAATGCCACCTTTTGACAGTG	CTGGATGCTCTCATCAGGACA
TGF-β	AGCTGGTGAAACGGAAGCG	GCGAGCCTTAGTTTGGACAGG
IL-4	GGTCTCAACCCCCAGCTAGT	GCCGATGATCTCTCTCAAGTGAT
GFAP	CGGAGACGCATCACCTCTG	AGGGAGTGGAGGAGTCATTCG
CD206	TCAGCTATTGGACGCGAGGCA	TCCGGGTTGCAAGTTGCCGT
c-Myc	ACCCGCTCAACGACAGCAGC	CCGTGGGGAGGACTCGGAGG
MBP	GGCCAGTAAGGATGGAGAGAT	CCTCTGAGGCCGTCTGAGA
P2Y12	GTGTTGACACCAGGCACATC	TCCCGGAGACACTCATATCC
MIP-2	CCAACCACCAGGCTACAGG	GCGTCACACTCAAGCTCTG
GAPDH	AGGTCGGTGTGAACGGATTTG	GGGGTCGTTGATGGCAACA
β-actin	GTGACGTTGACATCCGTAAAGA	GCCGGACTCATCGTACTCC

CHAPTER 3: RESULTS

3.1 Assessment of the Effects of Oral Administration of Clozapine or Pioglitazone on Remyelination 7 Days Following LPC-Mediated Demyelination

To assess the effects of clozapine and pioglitazone on remyelination in the LPC model, mice received bilateral stereotactic injections of LPC on one side and PBS on the opposite side of the corpus callosum and were administered treatment beginning 24 hours following surgery. In the first experiment, mice received daily oral treatment of either vehicle (distilled water, 5 ml/kg/day) or clozapine (10 mg/kg/day) by oral gavage (po) daily for 7 days. In the second experiment, mice received either vehicle (NEOBEE, 5 ml/kg/day; po) or pioglitazone (15 mg/kg/day; po) for 7 days. After these treatments for 7 days, brain sections that encompassed the rostral-caudal extent of the lesion were stained with eriochrome cyanine to visualize myelin and the volume of demyelination was determined by manually tracing the lesion border.

3.1.1 Mice treated with clozapine exhibited a similar volume of demyelination 7 days following LPC injection relative to vehicle-treated mice

Seven days after the injection of PBS and LPC in the corpus callosum of opposite hemispheres, LPC-induced lesion volumes were larger than those for PBS lesions in both vehicle- ($p = 0.025$) and clozapine-treated mice ($p = 0.011$) at day 7 (Figure 3E). However, LPC-induced lesion volumes were similar in size for vehicle-treated and clozapine-treated mice ($p = 0.982$).

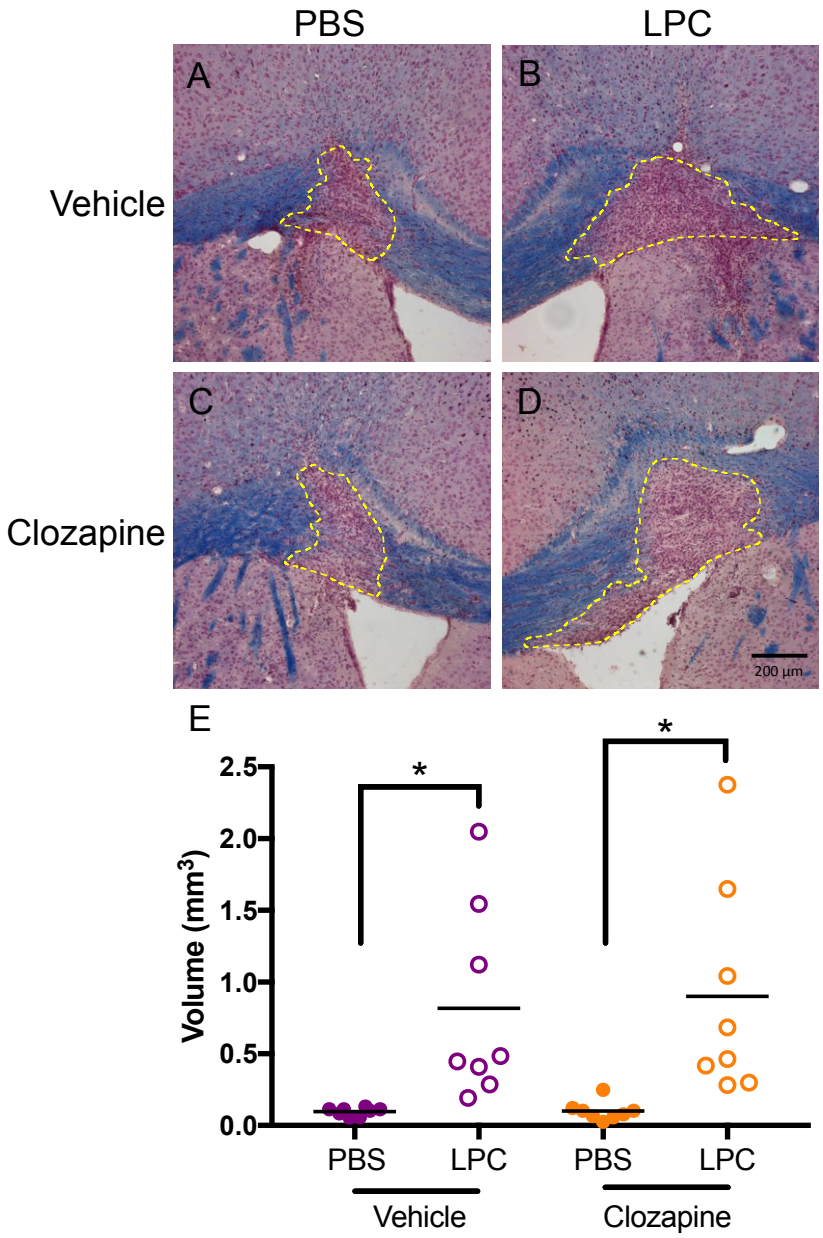

Figure 3. Mice treated with daily oral clozapine showed a similar volume of demyelination relative to vehicle-treated mice 7 days following LPC injection. Eriochrome cyanine (blue) and neutral red (pink) staining of PBS (A and C) and LPC (B and D) lesions in vehicle- and clozapine-treated mice 7 days following LPC injection. (E) Quantification of lesion volume, measured by tracing the cross-sectional area of demyelination on each section and calculating the area under the curve. Mice treated with clozapine showed comparable LPC lesion volumes relative to mice treated with vehicle (distilled water). LPC lesion volumes were much larger than the control PBS lesions in both treatment groups. Lesion volume is represented as mean ± SEM. *$p < 0.05$, a one-way ANOVA followed by Tukey's post hoc test. PBS = phosphate buffered saline, LPC = lysophosphatidylcholine.

3.1.2 Mice treated with pioglitazone exhibited a similar volume of demyelination 7 days following LPC injection relative to vehicle-treated mice

Seven days following the injection of PBS and LPC in the corpus callosum of opposite hemispheres, LPC-induced lesion volumes were larger than those for PBS lesions in both vehicle-treated ($p = 0.0039$) and pioglitazone-treated mice ($p < 0.0001$; Figure 4E). LPC lesions in pioglitazone-treated mice were marginally larger in volume relative to vehicle-treated mice, however, this difference did not reach statistical significance ($p = 0.0656$).

3.1.3 Daily oral treatment with pioglitazone produced comparable levels of activated macrophages/microglia within the lesion site 7 days following LPC injection relative to vehicle-treated mice

To determine whether pioglitazone altered the presence of activated macrophages/microglia within the lesion site following LPC injection, brain sections were immunohistochemically stained for the macrophage/microglia marker Iba1 and immunoreactivity was measured within the lesion site. Seven days following injection, the mean fluorescent intensity for Iba1 immunoreactivity was similar within the LPC lesions of vehicle- and pioglitazone-treated mice ($p = 0.669$; Figure 5E). In addition, levels of Iba1 immunoreactivity were similar within LPC and PBS lesions for both vehicle-treated ($p = 0.436$) and pioglitazone-treated mice ($p = 0.805$).

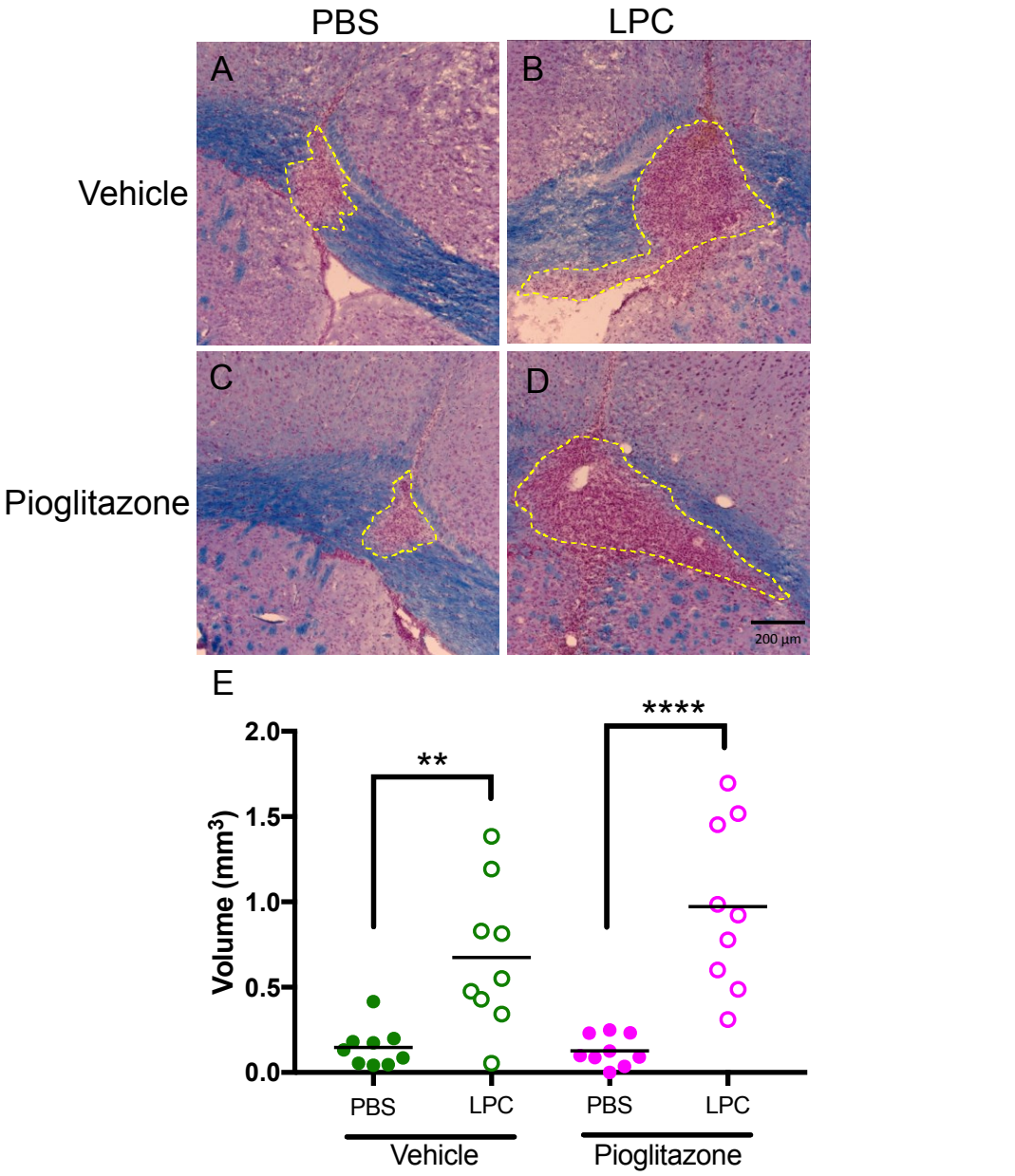

Figure 4. Mice treated with daily oral pioglitazone showed a similar volume of demyelination relative to vehicle-treated mice 7 days following LPC injection. Eriochrome cyanine (blue) and neutral red (pink) staining of PBS (A and C) and LPC (B and D) lesions in vehicle- and pioglitazone-treated mice 7 days following LPC injection. (E) Quantification of lesion volume measured by tracing the cross-sectional area of demyelination on each section and calculating the area under the curve. Mice treated with pioglitazone showed comparable LPC lesion volume relative to mice treated with vehicle (NEOBEE). LPC lesion volumes were much larger than the control PBS lesions in both treatment groups. Lesion volume is represented as mean ± SEM. **$p < 0.01$, ****$p < 0.0001$, a one-way ANOVA followed by Tukey's post hoc test. PBS = phosphate buffered saline, LPC = lysophosphatidylcholine.

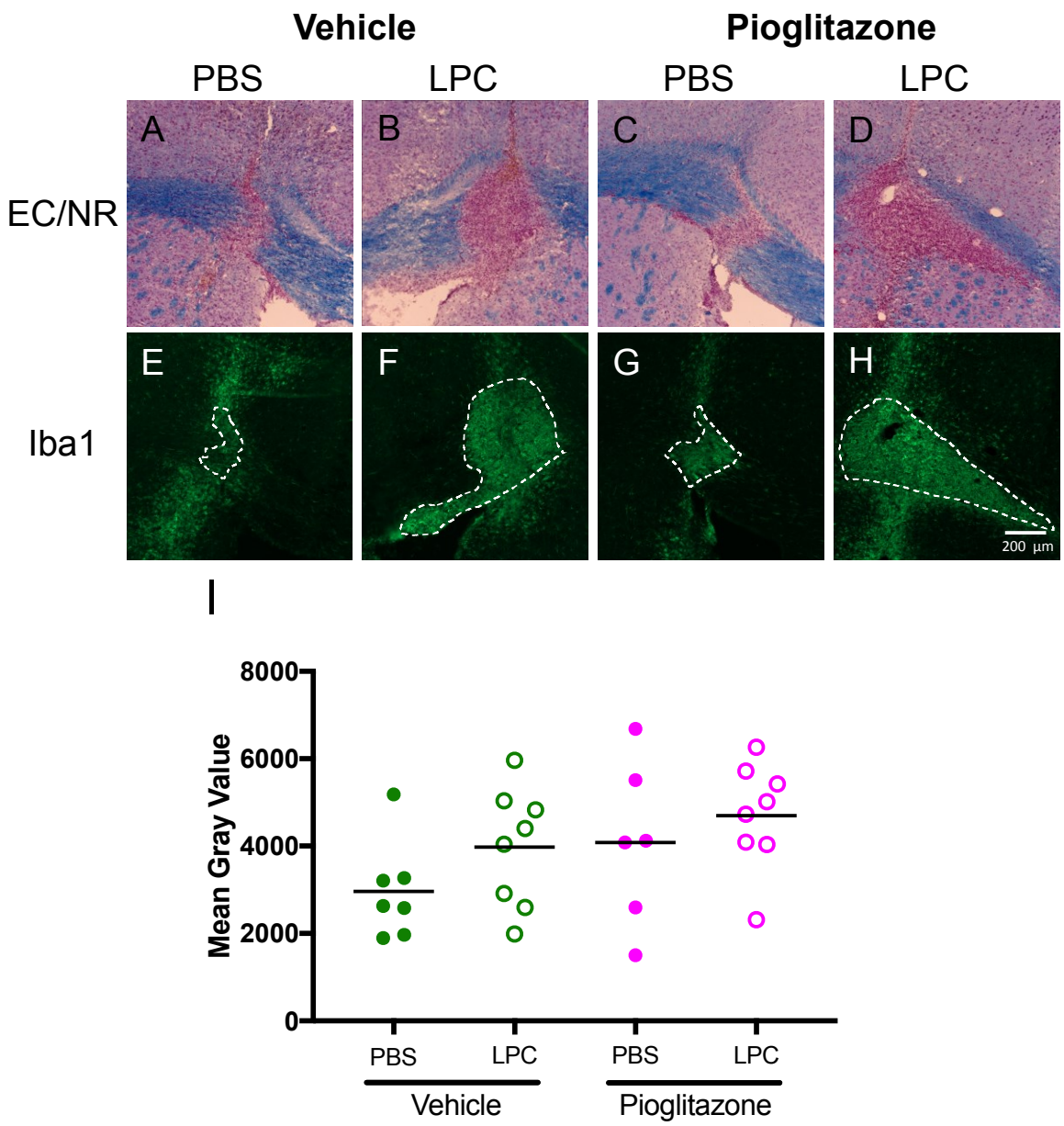

Figure 5. Daily oral pioglitazone treatment resulted in similar levels of activated microglia/macrophages within PBS and LPC lesions relative to vehicle 7 days following LPC injection. Representative micrographs of eriochrome cyanine/neutral red-stained brain sections (A-D) and adjacent fluorescent Iba1-stained brain sections (E-H) 7 days following LPC injection. (I) Quantification of the mean fluorescent intensity of Iba1 staining, measured by tracing the lesion border on the Iba1 image, using the adjacent eriochrome cyanine section as a reference, and taking the mean gray value using Image J. Mice treated with pioglitazone exhibited comparable levels of activated macrophages and microglia within the lesion site relative to vehicle-treated mice. Data represent mean ± SEM. One-way ANOVA followed by Tukey's post hoc test. PBS = phosphate buffered saline, LPC = lysophosphatidylcholine.

3.2 EAE Mice Showed a Smaller Volume of White Matter Loss 7 days, but not 14 Days, Following LPC Injection Relative to CFA/PTX Mice

To overcome limitations associated with autoimmune- and LPC-induced models of demyelination, PBS and LPC injections were performed on mice subjected to MOG_{35-55}-induced EAE or immunization controls that received CFA and pertussis toxin (PTX) injections but not MOG_{35-55} (CFA/PTX). Mice were euthanized 2, 7 and 14 days later and the brains were removed for myelin staining and quantitative image analysis. The volume of white matter loss was measured using a modified Cavalieri method of volume estimation.

3.2.1 EAE mice exhibited a similar peak volume of white matter loss 2 days following LPC injection relative to CFA/PTX mice

Two days following PBS and LPC injections into the corpus callosum of opposite hemispheres, LPC-mediated white matter loss was larger in volume relative to PBS-mediated white matter loss in both CFA/PTX mice ($p = 0.0007$) and EAE mice ($p = 0.0001$; Figure 6E). LPC-mediated volumes of white matter loss in EAE and CFA/PTX mice were similar ($p = 0.683$).

3.2.2 White matter loss mediated by LPC was smaller in EAE mice 7 days following injection relative to CFA/PTX mice

Seven days following injections of PBS and LPC into the corpus callosum, LPC-mediated white matter loss was larger than PBS-mediated white matter loss in both CFA/PTX ($p < 0.0001$) and EAE mice ($p = 0.0007$; Figure 7E). By contrast, EAE mice exhibited smaller LPC-mediated volumes of white matter loss compared to CFA/PTX mice ($p = 0.0004$).

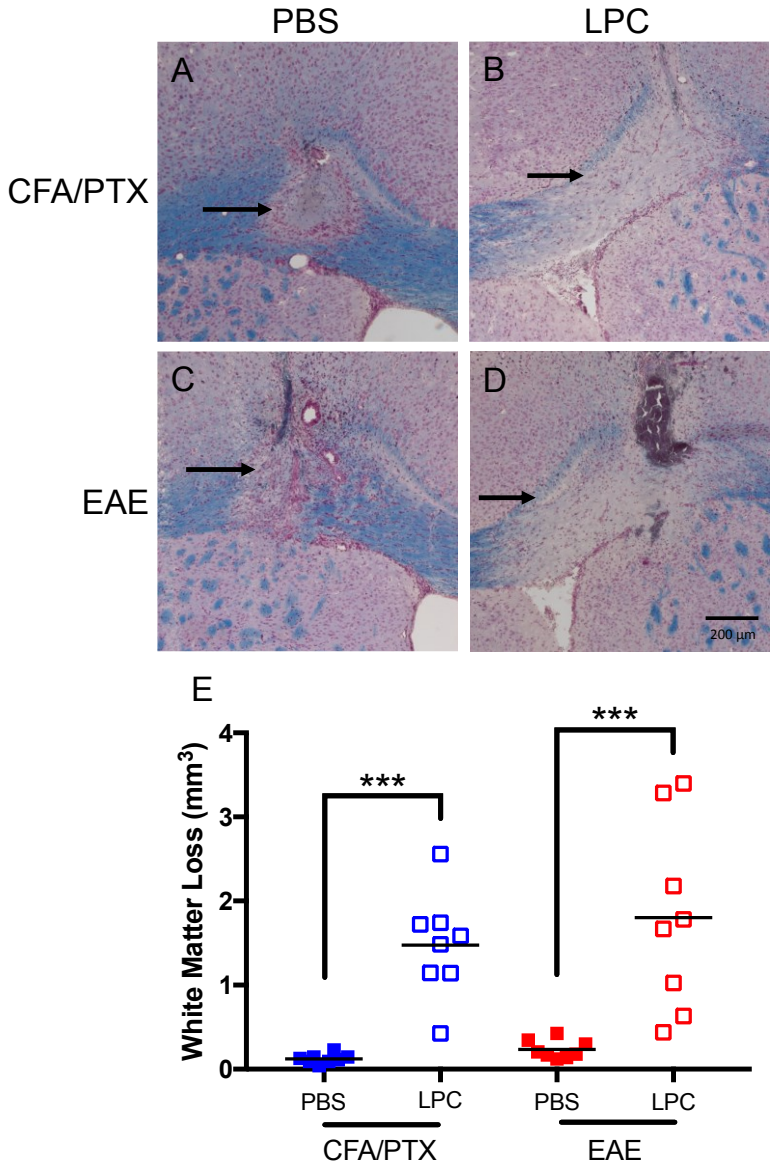

Figure 6. Two days following LPC injection, EAE mice exhibited similar peak volumes of LPC-induced white matter loss in the corpus callosum relative to CFA/PTX controls. Eriochrome cyanine (blue) and neutral red (pink) staining of PBS (A and C) and LPC (B and D) lesions in the corpus callosum of mice immunized with CFA alone and mice with EAE. (E) Quantification of volume of white matter loss within the corpus callosum 0.4 rostral and 1.2 mm caudal to the needle tracts. The cross-sectional area of white matter loss on each section was measured using a modified version of the Cavalieri method of volume estimation and calculating the area under the curve. LPC lesions in mice with EAE were similar in size to LPC lesions in CFA/PTX mice. LPC-induced white matter loss was much larger than the white matter loss in control PBS lesions in both treatment groups. White matter loss is represented as mean ± SEM. ***p<0.001, one-way ANOVA followed by Tukey's post hoc test. PBS = phosphate buffered saline, LPC = lysophosphatidylcholine.

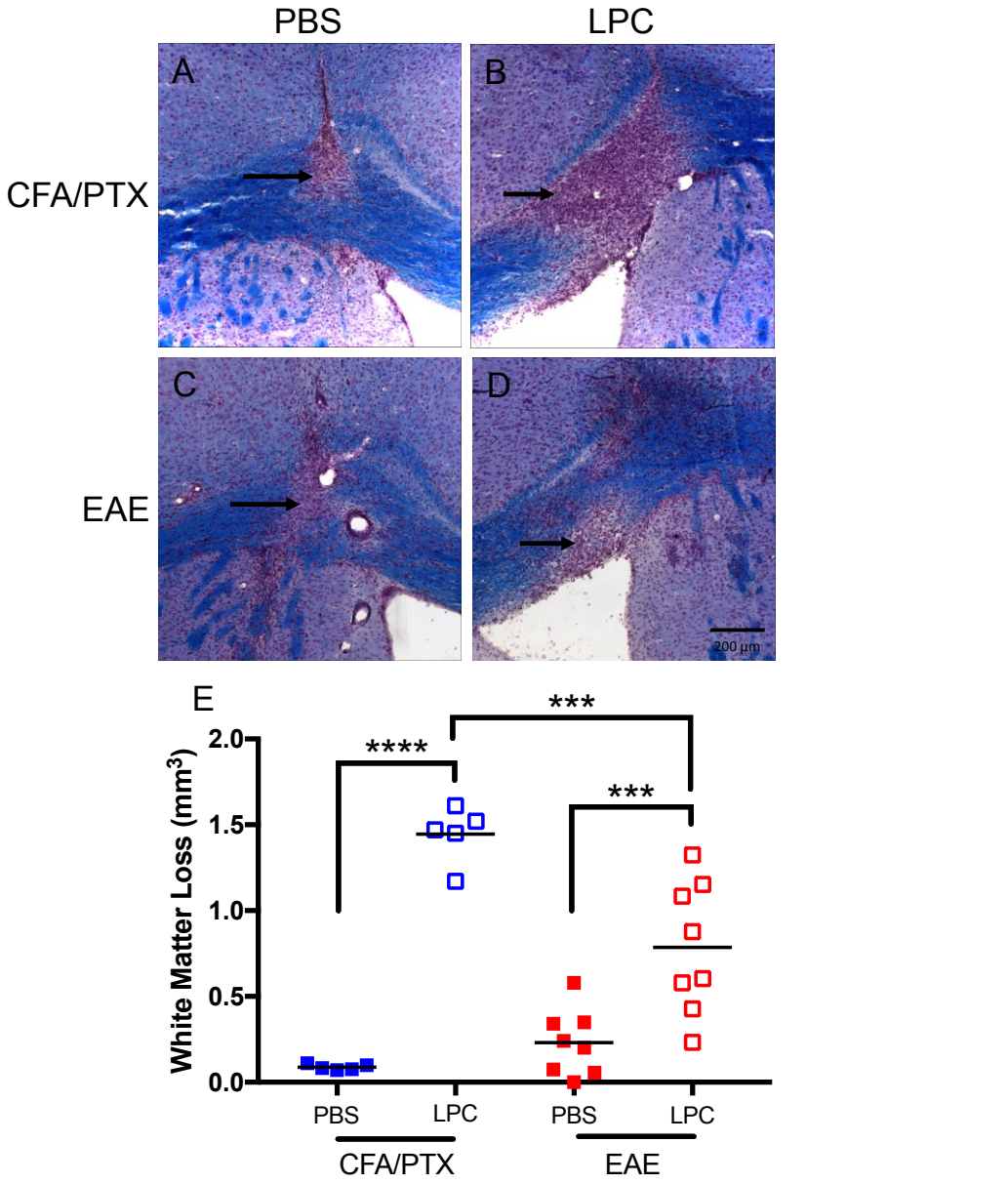

Figure 7. Seven days following LPC injection, EAE mice exhibited accelerated remyelination relative to CFA/PTX controls. Eriochrome cyanine (blue) and neutral red (pink) staining of PBS (A and C) and LPC (B and D) lesions in mice immunized with CFA alone and mice with EAE. (E) Quantification of volume of white matter loss within the corpus callosum extending 0.4 rostral and 1.2 mm caudal to the needle tracts. The cross-sectional area of white matter loss on each section was measured using a modified Cavalieri method of volume estimation and calculating the area under the curve. LPC-induced white matter loss was smaller in EAE mice relative to CFA/PTX mice. LPC-induced white matter loss was larger than the white matter loss in control PBS lesions for both treatment groups. White matter loss is represented as mean ± SEM. ***p < 0.001, ****p<0.0001, one-way ANOVA followed by Tukey's post hoc test. PBS = phosphate buffered saline, LPC = lysophosphatidylcholine.

3.2.3 White matter loss mediated by LPC injection was larger in EAE mice 14 days following injection relative to CFA/PTX mice

Fourteen days following injections of PBS and LPC into the corpus callosum, LPC-mediated white matter loss was larger than PBS-mediated white matter loss in EAE ($p = 0.0117$), but not CFA/PTX mice ($p = 0.284$; Figure 8E). EAE mice exhibited a larger volume of white matter loss compared to CFA/PTX mice ($p = 0.0295$).

3.3 EAE Mice Displayed an Accelerated Reduction in White Matter Loss Between Days 2 and 7 Following LPC Injection Relative to CFA/PTX Mice

To assess the temporal changes in demyelination, LPC-mediated white matter loss at each time point was compared for the CFA/PTX and EAE groups. CFA/PTX mice showed no change in white matter loss from days 2 to 7 ($p = 0.991$) but displayed a reduction in white matter loss from days 7 to 14 ($p = 0.0004$; Figure 9A). By contrast, EAE mice showed a reduction in LPC-mediated white matter loss from days 2 to 7 ($p = 0.0366$), indicative of enhanced remyelination. However, white matter loss volumes for EAE mice remained constant from days 7 to 14 ($p = 0.996$).

3.4 EAE Mice That Received an Injection of LPC into the Corpus Callosum Exhibited a Classical EAE Disease Course

When LPC was injected into the corpus callosum 7 days post-immunization (DPI), mice with EAE exhibited a classical disease course with symptom onset occurring between DPI 10-13 (Figure 9B). Peak disease severity occurred on DPI 17 followed by a gradual reduction in clinical scores. As expected, MOG_{35-55}

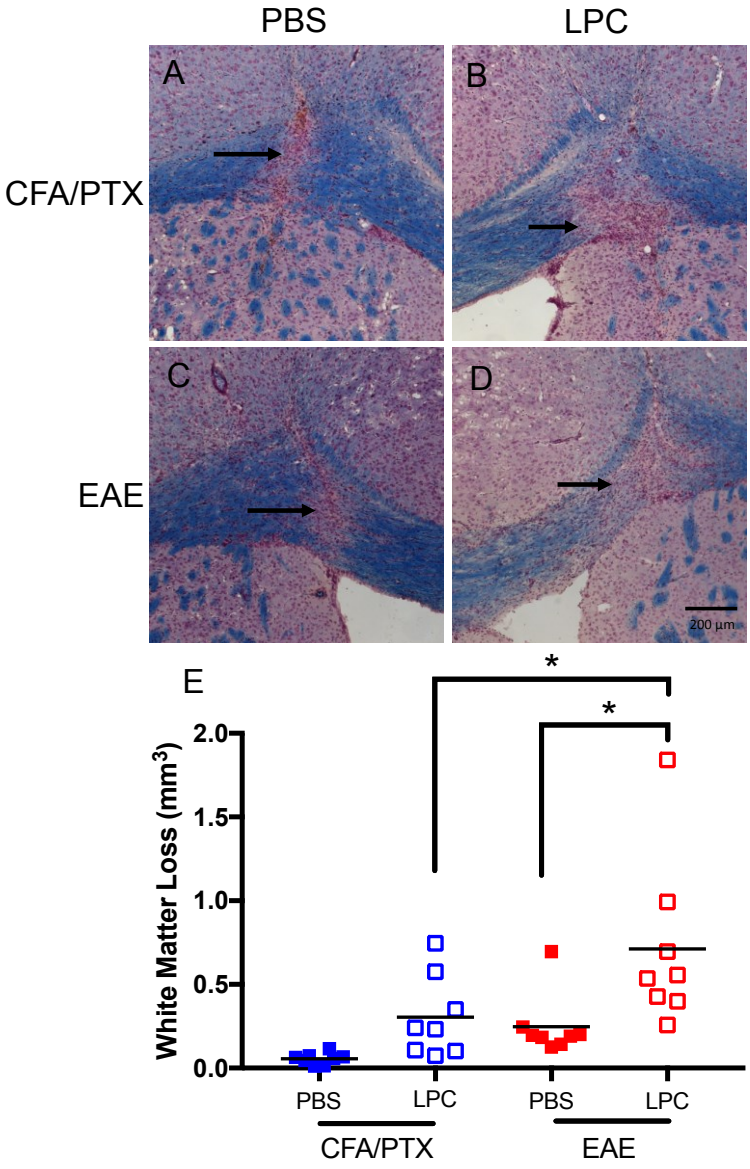

Figure 8. Fourteen days following LPC injection, EAE mice exhibited a larger volume of white matter loss in the corpus callosum relative to CFA/PTX controls. Eriochrome cyanine and neutral red staining of PBS (A and C) and LPC (B and D) lesions in mice immunized with CFA alone and mice with EAE. (E) Quantification of volume of white matter loss within the corpus callosum 0.4 rostral and 1.2 mm caudal to the needle tracts. The cross-sectional area of white matter loss on each section was measured using a modified Cavalieri method of volume estimation and calculating the area under the curve. Opposite to day 7, LPC-induced white matter loss was larger in mice with EAE relative to CFA/PTX mice. LPC-induced white matter lass was larger than the white matter loss in control PBS lesions in EAE, but not CFA/PTX mice. White matter loss is represented as mean ± SEM. *p < 0.05, one-way ANOVA followed by Tukey's post hoc test. PBS = phosphate buffered saline, LPC = lysophosphatidylcholine.

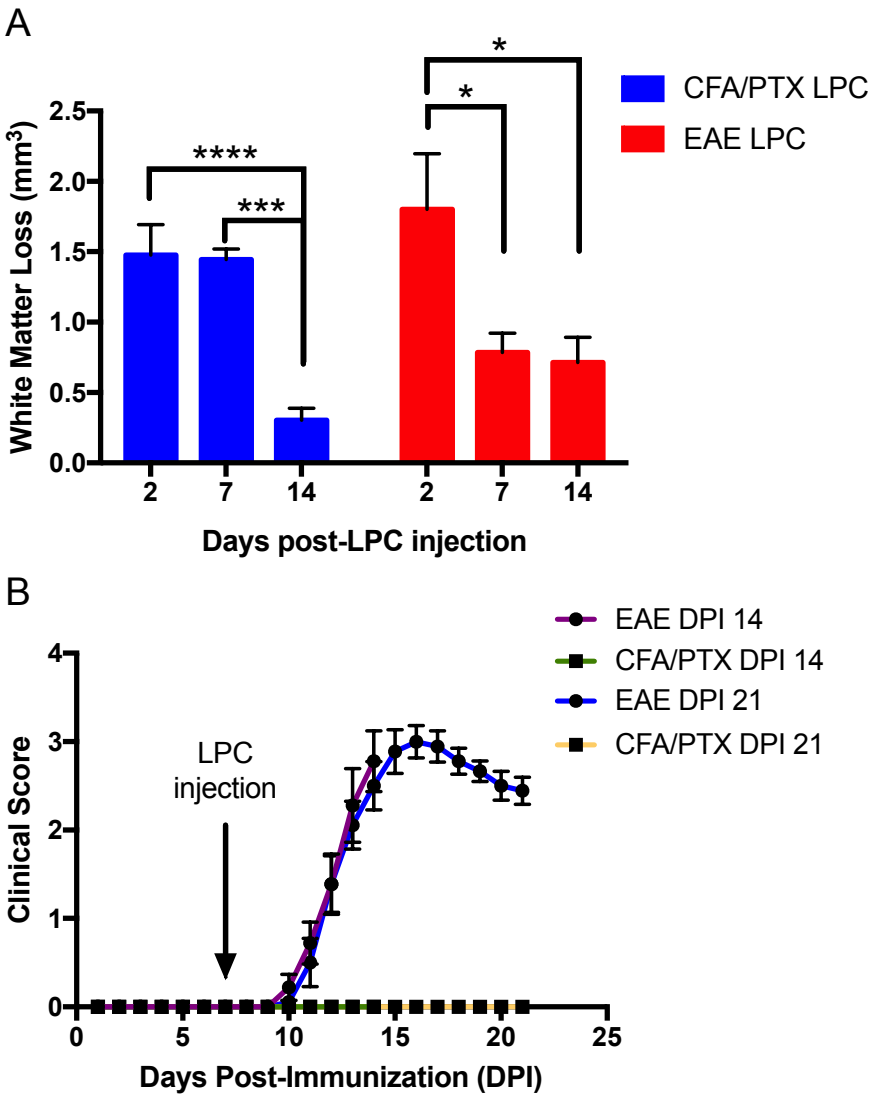

Figure 9. EAE mice recovered more quickly from LPC-induced demyelination than CFA controls and LPC-injected EAE mice exhibited a classical EAE disease course. (A) Mean volume of white matter loss within the corpus callosum 2, 7 and 14 days following LPC injection in CFA/PTX or EAE mice. LPC lesions in the corpus callosum of EAE mice showed a reduction in size between days 2 and 7, whereas no recovery occurred in CFA/PTX mice during this time. CFA/PTX mice exhibited a reduction in white matter loss between days 7 and 14, ultimately to a greater extent than EAE mice. (B) Clinical scores of EAE and CFA/PTX mice sacrificed 7 and 14 days following LPC injection (Days post-immunization 14 and 21, respectively). EAE mice exhibited a classical disease course, with disease onset occurring between days 10 and 13 and a gradual recovery beginning on day 17. Volume of pathology and clinical scores represented as mean ± SEM. *$p < 0.05$, ***$p < 0.001$, ****$p < 0.0001$, one-way ANOVA followed by Tukey's post hoc test. LPC = lysophosphatidylcholine.

immunization controls (CFA/PTX) that received an injection of LPC displayed no clinical signs of EAE.

3.5 Levels of Activated Macrophages/Microglia and Leukocytes were Similar in the Lesion Sites of EAE and CFA/PTX Mice

3.5.1 Seven days after LPC injection, activated macrophages/microglia and leukocytes were present at similar levels within the lesion sites of CFA/PTX and EAE mice

To determine whether the level of activated macrophages/microglia and leukocytes were different in CFA/PTX and EAE mice, brain tissue sections obtained at day 7 (DPI 14) were stained for Iba1 (macrophages/microglia marker) and CD45 (leukocyte marker) immunoreactivities within the lesion sites.

Seven days following injection, LPC lesions in CFA/PTX and EAE mice showed similar levels of both Iba1 ($p = 0.722$; Figure 10M) and CD45 ($p = 0.920$; Figure 10N) immunoreactivities. Iba1 levels in the PBS and LPC lesion sites for CFA/PTX ($p = 0.999$) and EAE mice ($p = 0.528$) were also similar (Figure 10M). However, CD45 immunoreactivity was elevated in the PBS lesion sites compared to LPC lesions of CFA/PTX mice ($p = 0.0173$), but not EAE mice ($p = 0.999$; Figure 10N).

3.5.2 Fourteen days after LPC injection, activated macrophages/microglia and leukocytes were present at similar levels in the lesion sites of EAE and CFA/PTX mice

To assess temporal changes in activated macrophage/microglia and leukocyte presence, tissue sections from day 14 (DPI 21) were assessed for levels of Iba1 and CD45 immunoreactivities within the lesion sites of CFA/PTX and EAE mice.

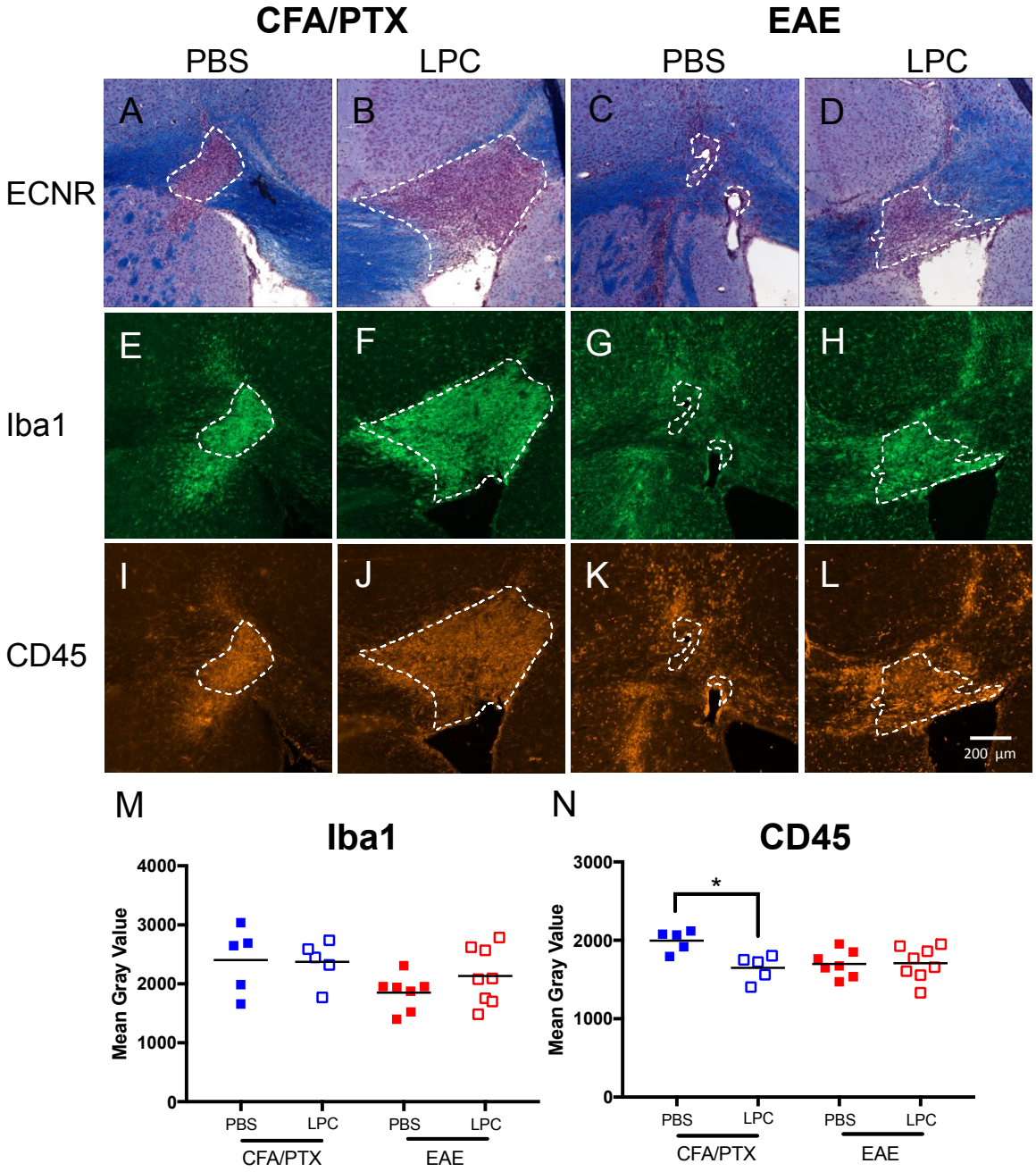
CFA/PTX
EAE
PBS
LPC
PBS
LPC
ECNR
Iba1
CD45
A
B
C
D
E
F
G
H
I
J
K
L
200 µm
M
Iba1
Mean Gray Value
4000
3000
2000
1000
0
PBS
LPC
PBS
LPC
CFA/PTX
EAE
N
CD45
Mean Gray Value
3000
2000
1000
0
*
PBS
LPC
PBS
LPC
CFA/PTX
EAE

Figure 10. Activated microglia/macrophages and leukocytes were present in similar levels at the lesion sites in CFA/PTX and EAE mice 7 days following LPC injection. Eriochrome cyanine staining of PBS and LPC lesions in CFA/PTX (A and B) and EAE (C and D) mice. Adjacent sections were double-labelled using antibodies against Iba1 (E-H) and CD45 (I-L) 7 days following LPC injection. Quantification of mean fluorescent intensity of $Iba1^+$ (M) and $CD45^+$ (N) cells. Mean fluorescent intensity was measured by tracing around the border of the lesion, using the eriochrome cyanine image as a reference, and taking the mean gray value determined by ImageJ. LPC lesions in CFA/PTX and EAE mice showed similar mean fluorescent intensities for both $Iba1^+$ and $CD45^+$ fluorescence. Leukocytes were present in higher levels in PBS lesions compared to LPC lesions for CFA/PTX mice only. Mean gray value is represented as mean ± SEM. *$p < 0.05$, one-way ANOVA followed by Tukey's post hoc test. PBS = phosphate buffered saline, LPC = lysophosphatidylcholine.

Fourteen days following the PBS and LPC injections, levels of Iba1 immunoreactivity were similar in PBS and LPC injection sites for CFA/PTX ($p = 0.895$) and EAE mice ($p = 0.473$; Figure 11M). CD45 immunoreactivity was also similar in the PBS and LPC lesions of CFA/PTX ($p = 0.239$) and EAE mice ($p = 0.493$; Figure 11N). LPC lesions in CFA/PTX and EAE mice showed comparable levels of both Iba1 ($p = 0.0985$; Figure 11M) and CD45 ($p = 0.978$; Figure 11N) staining.

3.6 Seven Days Following LPC Injection, Oligodendrocyte Precursor Cells are Present in Similar Levels in the Lesion Sites of EAE and CFA/PTX Mice

To assess whether the accelerated reduction in white matter loss observed in EAE mice was associated with an elevation in oligodendrocyte precursor cells (OPCs), tissue sections from day 7 (DPI 14) were immunohistochemically stained for NG2 and levels of immunoreactivity were measured within the lesion site. Seven days following injection, LPC lesions in EAE mice exhibited similar levels of NG2 compared to LPC lesions in CFA/PTX mice ($p = 0.428$; Figure 12I). NG2 immunoreactivity levels were also similar in the PBS and LPC lesions of CFA/PTX ($p = 0.983$) and EAE mice ($p = 0.809$).

3.7 Pro-Inflammatory Cytokine and Glial mRNA Levels were Elevated Following LPC Injection in EAE Mice

To assess the inflammatory profile of the lesion sites and surrounding parenchyma in CFA/PTX and EAE mice, the lesions areas were isolated 7 days following LPC injection and anti- and pro-inflammatory cytokine, glial and innate immune system mRNA levels were measured by qRT-PCR.

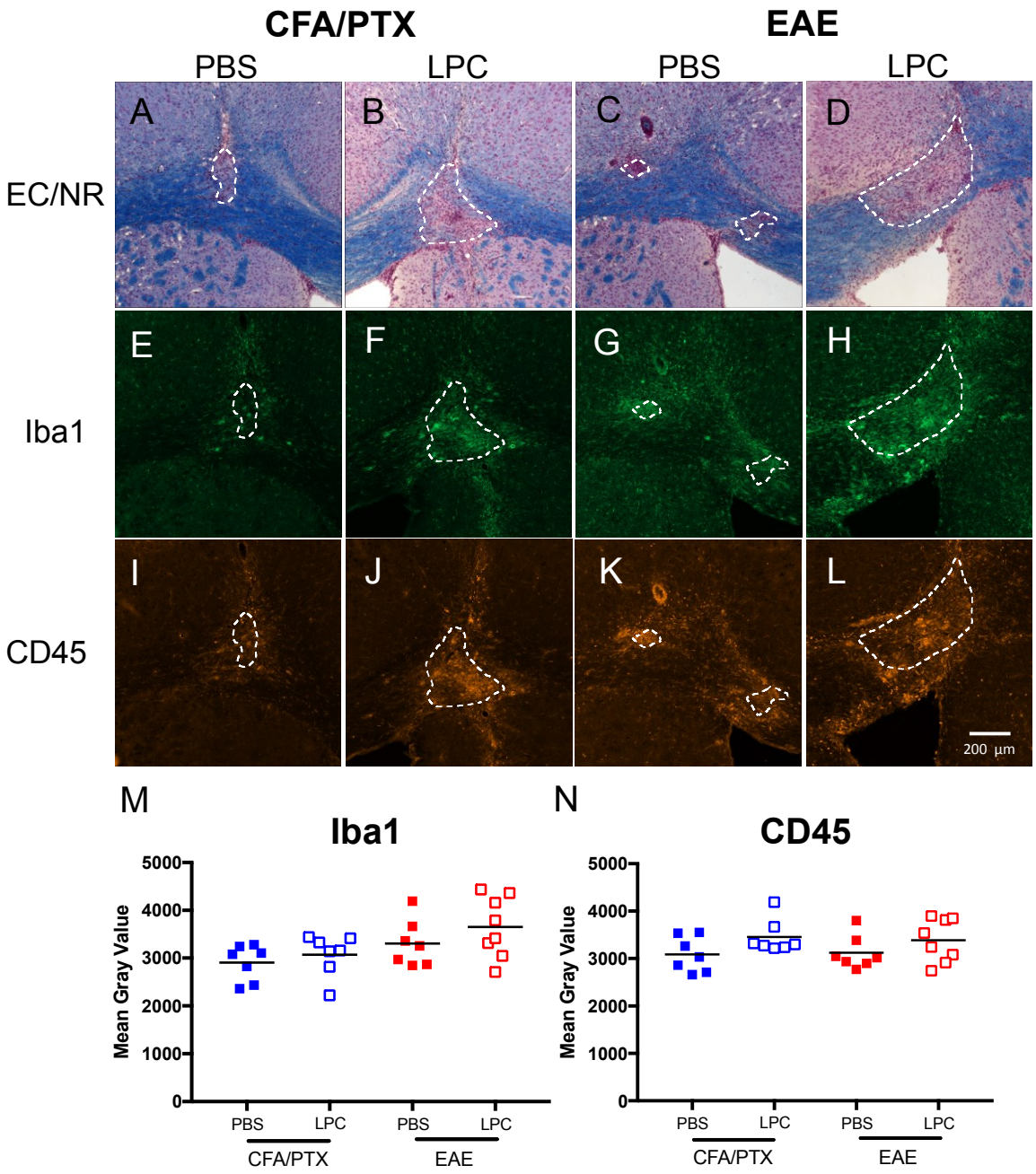
CFA/PTX
EAE
PBS
LPC
PBS
LPC
EC/NR
Iba1
CD45
A
B
C
D
E
F
G
H
I
J
K
L
200 µm
M
Iba1
Mean Gray Value
5000
4000
3000
2000
1000
0
PBS
LPC
PBS
LPC
CFA/PTX
EAE
N
CD45
Mean Gray Value
5000
4000
3000
2000
1000
0
PBS
LPC
PBS
LPC
CFA/PTX
EAE

Figure 11. Activated microglia/macrophages and leukocytes were present in similar levels at the lesion sites in CFA/PTX and EAE mice 14 days following LPC injection. Eriochrome cyanine staining of PBS and LPC lesions in CFA/PTX (A and B) and EAE (C and D) mice. Adjacent sections were double-labelled using antibodies against Iba1 (E-H) and CD45 (I-L) 7 days following LPC injection. Quantification of mean fluorescent intensity of $Iba1^+$ (M) and $CD45^+$ (N) cells. Mean fluorescent intensity was measured by tracing around the border of the lesion, using the eriochrome cyanine image as a reference, and taking the mean gray value determined by ImageJ. PBS and LPC lesions in CFA/PTX and EAE mice showed similar mean fluorescent intensities for both Iba1 and CD45 fluorescence. Mean gray value is represented as mean ± SEM. Data were analyzed using a one-way ANOVA followed by Tukey's post hoc test. PBS = phosphate buffered saline, LPC = lysophosphatidylcholine.

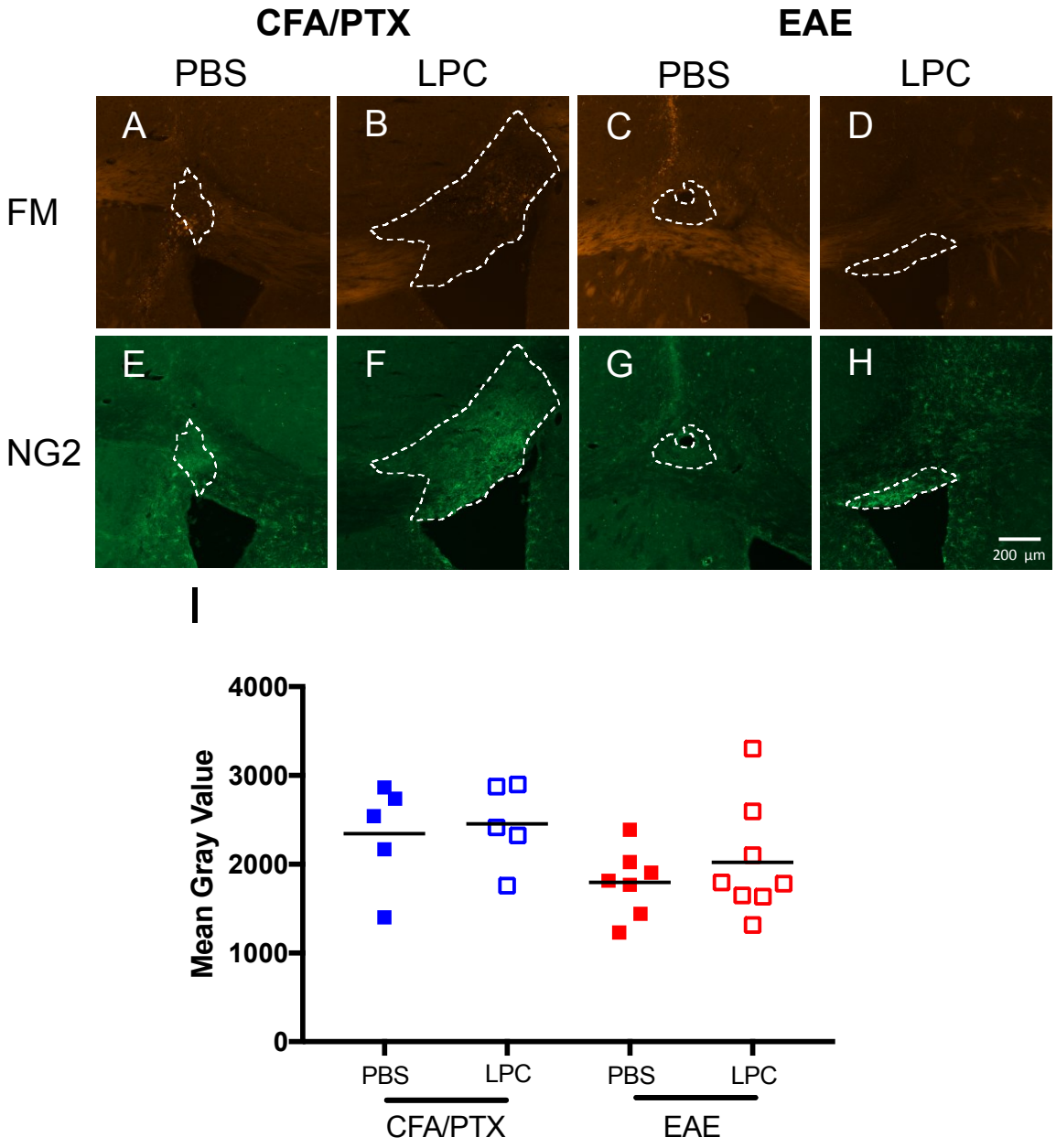

Figure 12. Oligodendrocyte precursor cells were present in similar levels in lesions in CFA/PTX and EAE mice. Representative micrographs of Fluoromyelin (A-D) staining and immunohistochemical staining using antibodies against NG2 (E-H) of PBS and LPC lesions in CFA/PTX and EAE mice. (I) Quantification of the mean fluorescent intensity of $NG2^{+}$ cells. Mean fluorescent intensity was measured by tracing the region of demyelination on the Fluoromyelin image, overlaying the trace onto the NG2 image and measuring the mean gray value using ImageJ. NG2 staining was present in comparable levels within the lesion sites in CFA/PTX and EAE mice. Mean gray value is represented as mean ± SEM. One-way ANOVA followed by Tukey's post hoc test. PBS = phosphate buffered saline, LPC = lysophosphatidylcholine.

3.7.1 Pro-inflammatory cytokine (IFN-γ, TNF-α, IL-6, IL-1β and TGF-β) mRNA levels were elevated in EAE mice 7 days following LPC injection

Seven days following LPC injection, mRNA levels for interferon gamma (IFN-γ) were elevated in the LPC lesions of EAE mice compared to LPC lesions in CFA/PTX mice ($p = 0.0002$) and PBS lesions in EAE mice ($p = 0.0125$; Figure 13A). Tumor necrosis factor alpha (TNF-α) mRNA levels were also elevated in the LPC lesions of EAE mice compared to LPC lesions in CFA/PTX mice ($p = 0.0003$) and PBS lesions in EAE mice ($p = 0.0141$; Figure 13B). Additionally, interleukin 6 (IL-6) mRNA levels were elevated in the LPC lesions of EAE mice compared to both LPC lesions in CFA mice ($p < 0.0001$) and PBS lesions in EAE mice ($p = 0.0004$; Figure 13C). Interleukin 1 beta (IL-1β) expression was also elevated in the LPC lesions of EAE mice compared to LPC lesions in CFA/PTX mice ($p = 0.0200$), but not compared to PBS lesions in EAE mice ($p = 0.396$; Figure 13D). Transforming growth factor beta (TGF-β) mRNA levels were increased in the LPC lesions of EAE mice relative to PBS lesions for EAE mice ($p = 0.0147$), but not LPC lesions in CFA/PTX mice ($p = 0.229$; Figure 13E).

3.7.2 mRNA encoding the anti-inflammatory cytokine IL-4 were present in similar levels in CFA/PTX and EAE mice 7 days following LPC injection

Levels of mRNA encoding interleukin 4 (IL-4) were similar in LPC lesions in EAE mice compared to both LPC lesions in CFA mice ($p = 0.994$) and PBS lesions in EAE mice ($p = 0.976$; Figure 13F).

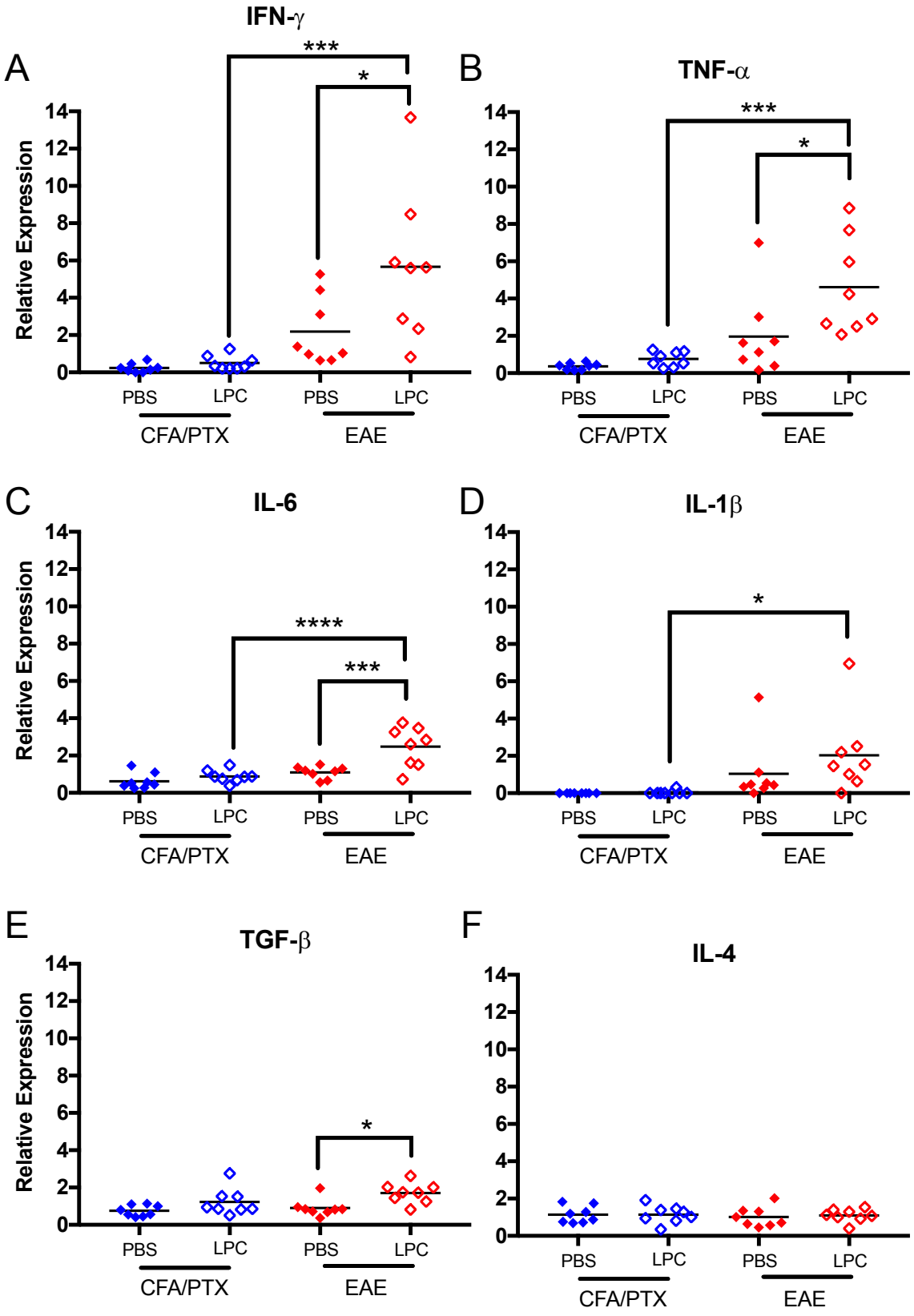
A
IFN-γ
***
*
B
TNF-α
***
*
C
IL-6
****
***
D
IL-1β
*
E
TGF-β
*
F
IL-4
Relative Expression
0
2
4
6
8
10
12
14
PBS
LPC
PBS
LPC
CFA/PTX
EAE

Figure 13. Levels of mRNA encoding several pro-inflammatory cytokines were elevated in EAE mice 7 days following LPC injection. Relative mRNA levels for various inflammatory cytokines in brain tissue (17-30 mg) 1 mm rostral and 2 mm caudal to the needle tracts, measured by qRT-PCR. mRNAs encoding IFN-γ (A), TNF-α (B) and IL-6 (C) in LPC lesions of EAE mice were elevated relative to both PBS lesions of EAE mice and LPC lesions of CFA/PTX mice. IL-1β (D) mRNA levels were elevated in LPC lesions of EAE mice relative to LPC lesions in CFA/PTX mice, while TGF-β (E) mRNA expression was elevated in LPC lesions relative to PBS lesions in EAE mice. Expression of IL-4 (F) mRNA was similar between EAE and CFA/PTX mice. Relative expression is represented as mean ± SEM. *$p < 0.05$, ***$p < 0.001$, ****$p < 0.0001$, one-way ANOVA followed by Tukey's post hoc test. PBS = phosphate buffered saline, LPC = lysophosphatidylcholine.

3.7.3 Levels of mRNA encoding the glial marker GFAP were elevated in EAE mice with a statistical trend for increased CD206 and MIP-2 mRNA levels 7 days following LPC injection

Seven days following LPC injection, glial fibrillary acidic protein (GFAP) mRNA levels were elevated in the LPC lesions of EAE mice compared to both LPC lesions in CFA/PTX mice ($p = 0.0003$) and PBS lesions in EAE mice ($p = 0.0006$; Figure 14A). There was a statistical trend for increased CD206 mRNA levels in the LPC lesions of EAE mice compared to LPC lesions in CFA/PTX mice ($p = 0.0517$), although this trend did not reach significance, but not compared to PBS lesions in EAE mice ($p = 0.684$; Figure 14B). There was also a statistical trend for increased macrophage inflammatory protein 2 (MIP-2) mRNA in the LPC lesions of EAE mice compared to LPC lesions in CFA/PTX mice ($p = 0.0794$), although this trend did not reach significance, but not compared PBS lesions in EAE mice ($p = 0.289$; Figure 14E).

3.7.4 mRNA encoding the glial markers c-Myc, MBP and P2Y12 were expressed at similar levels in CFA/PTX and EAE mice 7 days following LPC injection

Seven days following LPC injection, mRNA levels for c-Myc were similar in the LPC lesions of EAE mice compared to both LPC lesions in CFA/PTX mice ($p = 0.639$) and PBS lesions in EAE mice ($p = 0.196$; Figure 14C). However, c-Myc mRNA levels were elevated in the LPC lesions of CFA/PTX mice compared to PBS lesions in CFA/PTX mice ($p = 0.0392$). Myelin basic protein (MBP) mRNA levels were similar in the LPC lesions of EAE mice compared to both LPC lesions in CFA/PTX mice ($p = 0.996$) and PBS lesions in EAE mice ($p = 0.999$; Figure 14D). P2Y12 mRNA levels were similar in the LPC lesions of EAE mice

compared to both LPC lesions in CFA/PTX mice ($p = 0.649$) and PBS lesions in EAE mice ($p = 0.395$; Figure 14F).

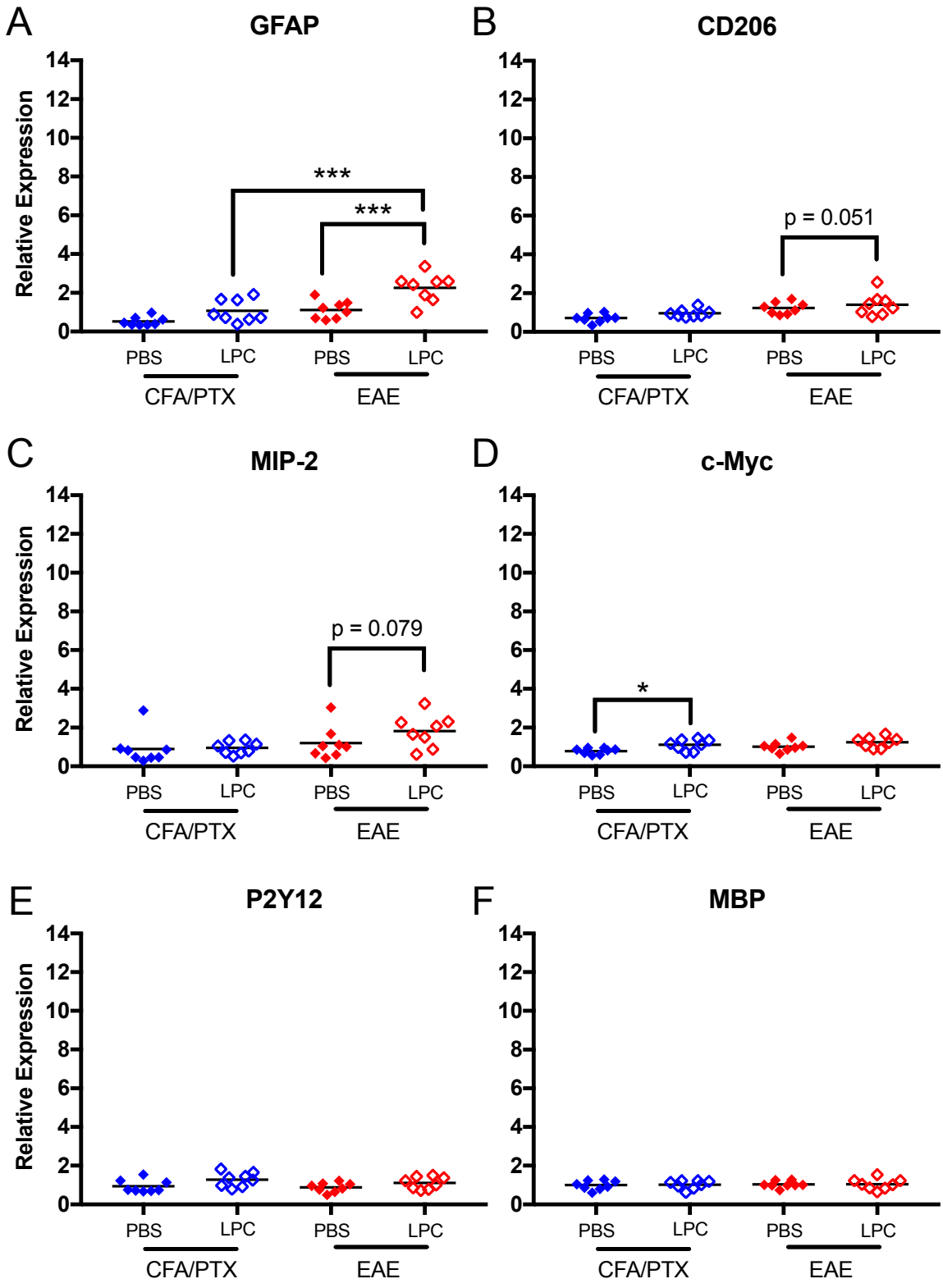
A
GFAP
B
CD206
C
MIP-2
D
c-Myc
E
P2Y12
F
MBP
Relative Expression
14
12
10
8
6
4
2
0
***
***
p = 0.051
p = 0.079
*
PBS
LPC
PBS
LPC
CFA/PTX
EAE

Figure 14. GFAP mRNA levels were elevated in EAE mice 7 days following LPC injection. Relative expression of various mRNAs encoding glial and innate immune cell markers in brain tissue (17-30 mg) 1 mm rostral and 2 mm caudal to the needle tracts, measured through qRT-PCR. mRNA encoding glial fibrillary acidic protein (GFAP; A) was elevated in LPC lesions of EAE mice relative to PBS lesions of EAE mice and to CFA/PTX mice. There was a trend in elevation of mRNA encoding CD206 (B) following LPC injection in EAE mice, however this trend did not reach statistical significance. There was also a trend in elevation of mRNA encoding macrophage inflammatory protein 2 (MIP-2; C) following LPC injection in EAE mice, however this trend did not reach statistical significance. Levels of mRNA encoding c-Myc (D) were elevated in LPC lesions compared to PBS lesions of CFA/PTX mice. Levels of mRNA encoding P2Y12 (E) and myelin basic protein (MBP; F) were comparable between CFA/PTX and EAE mice. Relative expression is represented as mean ± SEM. *$p < 0.05$, ***$p < 0.001$, one-way ANOVA followed by Tukey's post hoc test. PBS = phosphate buffered saline, LPC = lysophosphatidylcholine.

CHAPTER 4: DISCUSSION

4.1 Clozapine Fails to Promote Remyelination in the LPC Model of Focal Demyelination After Treatment for 7 Days

To determine the potential for clozapine to directly promote remyelination, clozapine (10 mg/kg/day, po) or vehicle (distilled water, 5 ml/kg/day, po) was administered for 7 days following injection of LPC into the corpus callosum. After 7 days, LPC lesions in vehicle-treated mice were similar in volume to clozapine-treated mice (Figure 3E).

Clozapine (10 mg/kg/day) has been shown to reduce EAE disease severity and improve behavioural and histological outcomes following cuprizone administration (O'Sullivan et al., 2014; Xu et al., 2010). However, the effects of clozapine in the LPC model have not been previously reported. In the few studies that have assessed clozapine in EAE, outcomes associated only with immunological function, and not myelination, were examined. In the cuprizone model, clozapine treatment was associated with a reduction in the loss of myelin markers (Xu et al., 2010). However, clozapine treatment was initiated at the same time as cuprizone administration, therefore it is unclear whether clozapine treatment protected from myelin loss or promoted remyelination. The present study demonstrates that oral clozapine treatment for 7 days does not enhance remyelination following LPC-mediated demyelination, however later timepoints should be assessed to determine whether administration of clozapine for longer than 7 days improved remyelination in this model.

4.2 Pioglitazone Fails to Promote Remyelination and May Exacerbate LPC-Mediated Demyelination After Treatment for 7 Days

To assess the capacity for pioglitazone to promote remyelination, pioglitazone (15 mg/kg/day) or vehicle (NEOBEE, 5 ml/kg/day) was administered for 7 days following injection of LPC into the corpus callosum. After 7 days, there was a statistical trend for increased LPC lesion size in pioglitazone-treated mice compared to LPC lesions for vehicle-treated mice (Figure 4E).

Pioglitazone, that is known to permeate the blood brain barrier (Grommes et al., 2013), has been shown to reduce EAE disease severity at doses of 5-10 mg/kg. This was associated with fewer infiltrating leukocytes and reduced demyelination at peak disease (Feinstein et al., 2002). However, spinal cord myelin was only assessed in EAE mice at peak disease, at which point remyelination had not begun. *In vitro*, pioglitazone promotes the differentiation of rodent OPCs to mature oligodendrocytes and improves the capacity of monocytes isolated from people with MS to phagocytose myelin (Bernardo et al., 2009; De Nuccio et al., 2011; Natrajan et al., 2015). Additionally, pilot clinical trials with small samples sizes have reported reduced disease severity following treatment with pioglitazone (Kaiser et al., 2009; Negrotto, Farez, & Correale, 2016).

The current study demonstrates that pioglitazone is unable to improve remyelination following LPC-mediated demyelination after treatment for 7 days. In fact, pioglitazone treatment resulted in a statistical trend in elevation of LPC lesion volume. To determine whether this elevation in lesion size could be

attributed to a difference in the density and activity of macrophages/microglia, brain sections were processed for the detection of Iba1 immunoreactivity.

Macrophages/microglia are required for remyelination following LPC-induced demyelination (Kotter et al., 2001). Therefore, an increase in LPC lesion volume may be associated with a reduction in macrophages/microglia. However, no difference was detected in the mean intensity of Iba1 staining within the LPC lesion sites between vehicle- and pioglitazone-treated mice (Figure 5I). Further investigation is required to determine how pioglitazone may exacerbate LPC-induced demyelination. Additionally, later timepoints in the time-course of LPC-mediated demyelination should be assessed to determine whether treatment with pioglitazone for longer than 7 days altered remyelination in this model.

4.3 Lesion Size is Smaller at Day 7, but Larger at Day 14, in EAE Mice Following LPC-Mediated Demyelination in the Corpus Callosum Relative to Controls

To characterize the effects of EAE on remyelination after LPC-induced demyelination, LPC was injected into the corpus callosum 7 days following immunization with either MOG_{35-55} emulsified in CFA (EAE group) and injected with PTX on days post-immunization (DPI) 0 and 2 or CFA alone plus PTX injections. This latter group served as an antigen control (CFA/PTX group). Brains were assessed 2, 7 and 14 days following LPC injection for white matter loss. Unexpectedly, EAE mice exhibited accelerated remyelination from day 2 to day 7 post-LPC injection. No further remyelination was detected at day 14 for

EAE mice (Figure 9A). By contrast, CFA/PTX mice did not show remyelination following LPC-induced demyelination until day 14. However, remyelination at day 14 was superior for CFA/PTX than EAE mice (Figure 9A). This suggests that while remyelination was accelerated in EAE mice, enhanced immune cell presence in the brain may have impaired the extent of myelin repair. A likely mechanism for reduced myelin repair in EAE mice is axonal loss secondary to autoimmune-mediated demyelination that depletes the pool of viable axons which can be remyelinated (Bjartmar, Wujek, & Trapp, 2003).

While the combination of LPC-mediated demyelination and EAE has not previously been reported, several studies have examined the effects of combining cuprizone-induced demyelination with EAE. Dietary administration of cuprizone, a copper chelator that suppresses the activity of copper-dependent enzymes that make myelin, for 6 weeks causes the selective death of oligodendrocytes (Torkildsen, Brunborg, Myhr, & Bø, 2008). Cuprizone administration for only 2 to 3 weeks leads to subtle biochemical deficits in forebrain myelin that are not sufficient to produce gross demyelination (Caprariello et al., 2018). Subclinical administration of cuprizone followed by EAE induction produces demyelination and peripheral immune infiltration in the forebrain, which is normally absent in EAE mice (Caprariello et al., 2018; Rüther et al., 2017; Scheld et al., 2016). These findings suggest that LPC-induced demyelination would attract myelin-reactive T cells, primed through EAE induction, to the corpus callosum, leading to enhanced demyelination.

4.3.1 Cellular infiltration is increased in the forebrain of EAE mice following LPC injection

To assess infiltration of peripheral immune cells into the forebrain, brain sections were immunohistochemically processed for the detection of Iba1 and CD45 - markers for macrophages/microglia and leukocytes, respectively. The mean intensity of these markers was not different within the lesion sites of EAE mice compared to CFA/PTX mice 7 days following LPC injection (Figure 10M and N). However, qualitatively, a diffuse pattern of innate immune cell activation and leukocyte infiltration was visible beyond the boundary of the PBS and LPC injection sites of EAE mice. Although not quantified, there appeared to be increased numbers of $Iba1^+$ (Figure 10G and H) and $CD45^+$ (Figure 10K and L) cells in the brain parenchyma surrounding both PBS and LPC lesions of EAE mice compared to CFA/PTX mice (Figure 10E, F, I and J). Unlike CFA/PTX mice, $CD45^+$ leukocytes were observed infiltrating the brain from blood vessels in EAE mice. These observations confirm that a stereotaxic injection into the forebrain leads to increased infiltration of leukocytes in EAE compared to CFA/PTX mice. However, instead of enhancing LPC-induced demyelination, increased innate immune cell activation and peripheral immune infiltration were associated with accelerated remyelination. These findings suggest that enhanced clearance of myelin debris and trophic support by activated immune cells may have stimulated remyelination. mRNAs encoding genes that regulate myelin repair were therefore measured in subsequent experiments. However, before describing these findings, the seemingly contradictory effects of cuprizone and LPC on remyelination in EAE should be addressed.

4.3.2 Systemic exposure to myelin antigens can reduce subsequent myelin reactivity

Contrary to studies previously described, Mana et al. (2009) described a profound reduction in EAE disease severity when MOG_{35-55} immunization occurred after dietary intake of cuprizone for 4 weeks followed by 2 weeks consuming normal laboratory chow. Cuprizone feeding alone led to increased myelin antigen reactivity of T and B cells in the cervical lymph nodes, but subsequent reduced reactivity after EAE induction. Suppressed EAE disease severity was accompanied by the near absence of inflammatory infiltrates in the cerebellum and spinal cord. These investigators postulated that cuprizone-induced systemic exposure to myelin antigens promoted a state of immune tolerance, marked by an elevation in anti-inflammatory cytokines and a reduction in pro-inflammatory cytokines, thereby limiting the immune response elicited by MOG_{35-55} immunization.

In EAE, myelin antigens and myelin-reactive leukocytes are also known to accumulate in the lymph nodes and spleen (van Zwam et al., 2009). Like cuprizone, this systemic exposure to myelin antigens through EAE induction may induce a state of tolerance towards myelin antigens and could explain why LPC-mediated demyelination does not lead to enhanced demyelination by MOG_{35-55}-primed cells.

4.3.3 Neurotrophins are produced by activated T cells

T cells reactive towards myelin antigens are present in similar levels in the blood of people with MS and healthy controls (Markovic-Plese et al., 1995), but those isolated from MS patients exist in an activated state (Zhang et al., 1994). Additionally, transfer of T cells isolated from EAE mice to naïve mice leads to the development of EAE in recipient mice that can often be more severe compared to the donor mice (Mannara et al., 2012). Consequently, autoimmunity has traditionally been considered a detriment to MS disease processes. However, studies have identified potentially beneficial implications of myelin-reactive T cells. Induction of myelin basic protein (MBP)-mediated EAE followed by surgical motor neuron axotomy reduces neuronal cell death in the rat spinal cord (Hammarberg et al., 2000). Moreover, intraperitoneal injection of activated MBP-reactive T cells suppresses injury and improves functional recovery following spinal cord contusion or optic nerve crush in rats (Hauben et al., 2000; Moalem et al., 1999). These benefits were attributed to the production of neurotrophins by activated lymphocytes (Hammarberg et al., 2000; Moalem et al., 2000). Neurotrophins are a class of cytokines known to promote neural cell survival and remyelination in EAE by blocking programmed cell death and overcoming metabolic deficits thought to drive disease progression in MS (Althaus, 2004; Linker et al., 2010; VonDran, Singh, Honeywell, & Dreyfus, 2011). Neurotrophin production by infiltrating myelin-reactive lymphocytes may therefore contribute to enhanced remyelination following LPC injection in EAE mice.

4.4 Accelerated Remyelination in EAE Mice is Accompanied by Increased Global Activation of Macrophages and Microglial Cells

Macrophages and microglia play critical roles in myelin injury and repair. As mentioned above, macrophages/microglia appear to be more abundant in the brain parenchyma surrounding the lesion sites 7 days following LPC injection in EAE, but not in CFA/PTX mice. Additionally, individual macrophages/microglia appear larger and more brightly stained (Figure 10G and H). By 14 days post-LPC injection, this trend remained, albeit to a lesser degree, while the densities of both $Ib1^+$ and $CD45^+$ cells within the lesion site were still similar between CFA/PTX and EAE mice (Figure 11M and N). Limitations in sensitivities of the immunohistochemical detection and quantification methods may have contributed to the failure to detect enhanced immune activation within the LPC injection sites of EAE mice. However, qRT-PCR measurements confirmed much greater expression of IFN-γ, TNF-α, IL-6 and IL-1β mRNA, all of which are expressed by macrophages/microglia (Arellano, Ottum, Reyes, Burgos, & Naves, 2015; Lévesque et al., 2016; Renno, Krawkoski, Piccirillo, Lin, & Owens, 1995; Samoilova, Horton, Hilliard, Liu, & Chen, 1998) in the LPC injected hemispheres of EAE mice compared to CFA/PTX mice (Figure 13A, B, C and D), which supports the observation of enhanced activation of these cells.

There is ample evidence for the beneficial role of macrophages/microglia following LPC-mediated demyelination. Macrophages/microglia are rapidly recruited and activated following LPC injection, after which these cells phagocytose myelin debris (Ousman & David, 2000). Peripheral depletion of

monocytes before LPC injection leads to impaired clearance of myelin, which is also associated with reduced OPC recruitment and impaired remyelination (Kotter et al., 2001; Kotter, Zhao, Van Rooijen, & Franklin, 2005; Triarhou & Herndon, 1985). Artificial activation and stimulation of macrophages/microglia leads to enhanced remyelination following LPC injection (Doring et al., 2015). Resident microglia and infiltrating macrophages are activated in EAE and play an integral role in disease pathogenesis (Bjelobaba, Begovic-Kupresanin, Pekovic, & Lavrnja, 2018). This suggests that the accelerated remyelination observed following LPC injection in EAE mice may be due to enhanced phagocytic activity by macrophages/microglia activated through EAE induction.

4.4.1 Macrophage/microglia polarization

To determine whether macrophages/microglia in the forebrain displayed polarization following LPC injection in EAE mice, the expression of various markers was measured by qRT-PCR 7 days following LPC injection. There was a statistical trend for the elevation of mRNAs encoding CD206 (Figure 14B) and macrophage inflammatory protein-2 (MIP-2; Figure 14C) in LPC lesions relative to PBS lesions in EAE mice. Levels of mRNA encoding c-Myc (Figure 14D) and P2Y12 (Figure 14E) were similar in CFA/PTX and EAE mice.

CD206, c-Myc and P2Y12 are markers for alternatively activated (M2) macrophages/microglia, which exert anti-inflammatory effects and are known to phagocytose myelin (Boven et al., 2006). While CD206 was the only marker that

showed a statistical trend for increased expression, this elevation in conjunction with accelerated remyelination suggest that M2-polarized macrophages/microglia may contribute to remyelination through enhanced myelin phagocytosis in this dual model. However, further analysis is required to assess the phagocytic activity of macrophages/microglia in this LPC-EAE model.

MIP-2 is a pro-inflammatory chemokine associated with classically activated (M1) macrophages/microglia that facilitates the migration of leukocytes (Wolpe et al., 1989). A statistical trend in the elevation of mRNA encoding MIP-2 in LPC lesions in EAE mice is consistent with the observation of increased leukocyte infiltration into the brain parenchyma in EAE mice and suggests that this chemotactic signal may be higher following LPC compared to PBS injection.

4.5 Markers of Remyelination

4.5.1 Oligodendrocyte precursor cells

To determine whether enhanced remyelination was associated with an increased number of oligodendrocyte precursor cells (OPCs), brain sections were assessed for NG2 immunoreactivity. $NG2^+$ cells were present at similar levels within the lesion site of CFA/PTX and EAE mice (Figure 12I). By 7 days following LPC injection, remyelination was complete in EAE mice. These findings suggest that an elevation in OPC number may only be apparent earlier in lesion progression.

4.5.2 Myelin basic protein

To assess the production of myelin by oligodendrocytes, qRT-PCR was performed on the lesions and surrounding brain parenchyma 7 days following LPC injection. mRNA encoding myelin basic protein (MBP) was present at similar levels in CFA/PTX and EAE mice (Figure 14F). Enhanced remyelination requires increased production of myelin components. However, myelin production is limited to the oligodendrocytes within the lesion and therefore only comprises a small fraction of the cells assessed by qRT-PCR. Therefore, the signal was likely subject to pool dilution effects. Additionally, remyelination was relatively complete by 7 days following LPC injection in EAE mice. To detect markers associated with remyelination, an earlier timepoint should therefore be analyzed.

4.6 Patterns of Cytokine mRNA Induction are Suggestive of the Activation of Myelin Repair after LPC injection in EAE Mice

4.6.1 Expression of pro-inflammatory genes is enhanced in LPC lesions of EAE mice

To assess the mRNA levels for various cytokines, qRT-PCR analysis was conducted on the lesions and surrounding brain parenchyma 7 days following LPC injection. mRNAs encoding interferon gamma (IFN-γ; Figure 13A), tumor necrosis factor alpha (TNF-α; Figure 13B) and interleukin 6 (IL-6; Figure 13C) were elevated in the LPC lesions of EAE mice relative to both PBS lesions in EAE mice and LPC lesions in CFA/PTX mice. These findings demonstrate that elevated mRNA levels resulted from the combination of LPC and EAE and were not simply produced by injury from a stereotaxic injection in EAE.

TNF-α is a pleiotropic cytokine that is produced at high levels by microglia, macrophages and other infiltrating leukocytes in EAE (Renno, Krakowski, Piccirillo, Lin, & Owens, 1995). Binding of soluble TNF-α to TNF receptor 1 (TNFR1) has been implicated in facilitating disease progression, whereas binding of transmembrane TNF-α to TNF receptor 2 (TNFR2) has protective effects (Alexopoulou et al., 2006; Brambilla et al., 2011; Eugster et al., 1999). Additionally, binding of transmembrane TNF-α to TNFR2, which is expressed on oligodendrocytes and macrophages/microglia, is integral to the induction OPC differentiation necessary for remyelination following cuprizone-mediated demyelination (Arnett et al., 2001; Madsen et al., 2016). The elevation in TNF-α mRNA observed in the LPC lesions of EAE mice may contribute to accelerated remyelination by TNFR2 activation that stimulates the differentiation of OPCs.

Interferon gamma (IFN-γ), produced by T cells, natural killer (NK) cells and macrophages, plays a stage-specific role in the progression of EAE (Arellano et al., 2015). It has been shown to drive the induction phase of EAE by facilitating lymphocyte entry into the CNS, activation of macrophages and stimulation of pro-inflammatory cytokine production (Furlan et al., 2001; Olsson, 1995; Sonar, Shaikh, Joshi, Atre, & Lal, 2017). In the chronic phase of EAE, IFN-γ aids disease resolution by inducing the apoptotic death of T cells (Furlan et al., 2001). Mice lacking interleukin 6 (IL-6) are highly resistant to the development of EAE, indicating this cytokine is required for the induction phase of EAE. (Mendel, Katz, Kozak, Ben-Nun, & Revel, 1998; Samoilova et al., 1998). Although IFN-γ and IL-6

appear to have predominantly pro-inflammatory roles 14 days following EAE induction, these cytokines may still assist the resolution of LPC-mediated demyelination. The elevation of cytokines that promote the transmigration of peripheral immune cells primed for myelin repair into the CNS may also have contributed to accelerated remyelination in EAE mice.

Many studies have implicated pro-inflammatory cytokines in the pathogenesis of EAE (Batoulis et al., 2014; Eugster, Frei, Kopf, Lassmann, & Fontana, 1998; Sonar et al., 2017). However, there is evidence that inflammation facilitates remyelination. Using a strain of rats that display progressive myelin loss over their lifespan, Foote and Blakemore (2005) demonstrated that OPCs transplanted into the spinal cord performed only minimal remyelination around the site of transplantation. Subsequent injection of saline distal to the transplantation site to induce a local inflammatory response stimulated remyelination by the transplanted OPCs. This illustrates the potential for inflammation traditionally considered detrimental to facilitate remyelination.

4.6.2 Interleukin 1 beta mRNA is elevated in the EAE forebrain following stereotaxic injection

Interleukin 1 beta (IL-1β) is a cytokine produced by peripheral immune cells that is known to drive EAE pathogenesis (Lévesque et al., 2016; Lin & Edelson, 2017). While generally considered pro-inflammatory, mice lacking IL-1β displayed impaired remyelination following cuprizone-induced demyelination (Mason, Suzuki, Chaplin, & Matsushima, 2001). IL-1β mRNA levels were elevated to the

same extents by injection of PBS or LPC in EAE mice over CFA/PTX mice (Figure 13D). Therefore, IL-1β mRNA is likely increased in the forebrain of EAE mice by the trauma associated with a stereotaxic injection rather than being a response specific to LPC-induced demyelination.

4.6.3 Transforming growth factor beta mRNA is elevated to similar extents by LPC injections in EAE and CFA/PTX mice

Transforming growth factor beta (TGF-β) is known to promote the resolution of EAE (Smith, Kono, & Theofilopoulos, 1991) and stimulate the production of hepatocyte growth factor that increases remyelination (Lalive et al., 2005). Consistent with a permissive role in accelerated remyelination in EAE mice, TGF-β mRNA levels were elevated following LPC injection relative to PBS injection in EAE mice (Figure 13E). Hence, TGF-β may also play a role in stimulating remyelination following LPC-induced white matter loss in EAE mice.

4.6.4 Interleukin 4 mRNA expression is similar in forebrain lesions of CFA/PTX and EAE mice

Interleukin 4 (IL-4) is an anti-inflammatory cytokine primarily produced by microglia and is associated with the recovery phase of EAE (Khoury, Hancock, & Weiner, 1992; Ponomarev, Maresz, Tan, & Dittel, 2007). Delivery of IL-4 directly into the cerebrospinal fluid (CSF) of EAE mice after disease onset reduces disease severity, spinal cord demyelination and axonal loss (Casella et al., 2016). IL-4 expression does not begin until later in the EAE disease course, where it is associated with disease resolution, likely through polarizing

macrophages/microglia to an M2 phenotype (Khoury et al., 1992; Ponomarev et al., 2007; Rawji & Yong, 2013). Gene expression was measured 7 days post-LPC injection (14 days post-EAE induction) to assess whether accelerated remyelination in EAE mice was associated with an earlier production of IL-4. However, IL-4 mRNA levels were similar in CFA/PTX and EAE mice (Figure 13F), suggesting IL-4 is not a major driver of remyelination in this dual model.

4.7 GFAP Gene Expression is Elevated Following LPC Injection in EAE Mice

Glial fibrillary acidic protein (GFAP) is a marker for reactive astrocytes, which are present within LPC lesions (Lau et al., 2012). GFAP mRNA levels were elevated in LPC lesions of EAE mice 7 days following injection relative to both PBS lesions in EAE mice and LPC lesions in CFA/PTX mice (Figure 14A). This suggests that EAE enhances astrocyte activation in the LPC lesions of EAE mice. Astrocytes may contribute to remyelination in several ways, which include providing trophic support to glial cells, facilitating OPC migration and enhancing oligodendrocyte survival (Kıray, Lindsay, Hosseinzadeh, & Barnett, 2016).

4.8 LPC-Mediated Demyelination in EAE Mice as a Model for MS

The dual LPC and EAE model simulates a demyelinating event in the context of an established myelin-reactive immune response. Instead of contributing to further demyelination, the inflammatory conditions of EAE accelerate remyelination in the corpus callosum. Remyelination frequently occurs in lesions that appear early in the MS disease course, but is diminished in the chronic

phase of the disease (Goldschmidt et al., 2009). This dual model may therefore represent the conditions observed during a relapse early in the MS disease course. More detailed analysis of the cell populations present within the LPC lesions of EAE mice should reveal additional information about the factors contributing to remyelination in a pro-inflammatory context. Based on these findings, it may be possible to employ pharmacological and gene targeting approaches to identify the processes that mediate accelerated remyelination in EAE mice.

4.9 Limitations and Future Directions

Clozapine and pioglitazone were unable to promote remyelination following LPC-induced demyelination after treatment for 7 days. However, brain and serum levels of these drugs should be measured at the time of sacrifice to confirm adequate dosing and delivery.

Further experimentation is also required to characterize the dual LPC and EAE model. Preliminary analysis suggests that enhanced remyelination following LPC injection may be driven by increased myelin phagocytosis by M2-polarized macrophages/microglia, as evidenced by increased global activation of parenchymal macrophages/microglia and a statistical trend in elevated mRNA levels of the M2 marker CD206. Because remyelination is relatively complete by 7 days post-LPC injection in EAE mice, markers for enhanced phagocytosis would likely be absent or diminished at this point, as myelin phagocytosis

precedes remyelination. Additionally, the pro-inflammatory cytokine profile detected may not represent the conditions in which remyelination occurred and may instead represent a shift towards a pro-inflammatory phase that is actually inhibitory towards remyelination, as no remyelination occurred in EAE mice between days 7 and 14 (Figure 9A). Therefore, an earlier timepoint, such as 4 days post-LPC injection, should be examined using immunohistochemistry and qRT-PCR to better understand the conditions that facilitate remyelination in this model.

A limitation of this study is that analysis of healthy mice and non-injected, naive EAE mice was not conducted. It would be beneficial to assess baseline gene expression of inflammatory markers in both such control groups. However, due to minimal involvement of the forebrain in EAE, it is expected that leukocyte markers and pro-inflammatory cytokine expression and would be very low in both.

For qRT-PCR analysis, the brain parenchyma immediately surrounding the corpus callosum lesions was included. Therefore, a pool dilution effect may have masked the detection of markers expressed by small cell populations localized within the lesions, such as oligodendrocytes or polarized macrophages/microglia. The corpus callosum could be dissected from surrounding brain tissue, however this may result in missing portions of the lesion or including an inconsistent

quantity of tissue between mice. Therefore, more sensitive methods, such as fluorescence-activated cell sorting should be used.

To explore the effects of different inflammatory profiles on the response to LPC-mediated demyelination, LPC should be injected at different points in the EAE disease course. In the current study, LPC was injected before mice experience EAE clinical symptoms. Injection of LPC at peak disease severity or during the recovery phase of EAE or in a relapsing model of EAE would provide insight into the inflammatory factors affecting remyelination both in an acute and chronic context.

4.10 Conclusions

The overarching objectives of this study were two-fold: 1) To determine the potential for clozapine and pioglitazone to promote remyelination following LPC-mediated demyelination, and 2) To characterize the combination of LPC-mediated demyelination and EAE.

Both clozapine and pioglitazone were unable to promote remyelination following LPC-mediated demyelination in the corpus callosum after 7 days of treatment. Previous cell-based and animal studies suggest these drugs may promote remyelination in MS (Bernardo et al., 2009; Feinstein et al., 2002; Natrajan et al., 2015; O'Sullivan et al., 2014; Xu et al., 2010). However, this study was unable to

demonstrate that these compounds directly promote remyelination within the timeframe studied.

This is the first study to suggest accelerated remyelination following LPC-mediated demyelination in the corpus callosum of mice with EAE, despite increased cellular infiltration into the forebrain and enhanced pro-inflammatory gene expression. Increased macrophage infiltration and microglial activation may accelerate remyelination by increasing myelin phagocytosis (Doring et al., 2015; Kotter et al., 2001, 2005). Elevated pro-inflammatory cytokine expression may contribute to remyelination by facilitating leukocyte entry into the CNS (IFN-γ and IL-6) and through promoting OPC recruitment (TNF-α). While further experimentation is required to characterize this phenomenon, this dual model may simulate a relapse early in the disease course of MS, where remyelination is frequently observed, and therefore allow for the identification of mechanisms inherent to MS that can be manipulated to enhance remyelination.

REFERENCES

Alexopoulou, L., Kranidioti, K., Xanthoulea, S., Denis, M., Kotanidou, A., Douni, E., … Kollias, G. (2006). Transmembrane TNF protects mutant mice against intracellular bacterial infections, chronic inflammation and autoimmunity. *European Journal of Immunology*, *36*(10), 2768–2780. https://doi.org/10.1002/eji.200635921

Althaus, H. H. (2004). Remyelination in multiple sclerosis: A new role for neurotrophins? *Progress in Brain Research*, *146*, 415–432. https://doi.org/10.1016/S0079-6123(03)46026-3

Alvir, J. M. J., Lieberman, J. A., Safferman, A. Z., Schwimmer, J. L., & Schaaf, J. A. (1993). Clozapine-induced agranulocytosis; Incidence and risk factors in the United States. *New England Journal of Medicine*, *329*(2), 162–167.

Ardekani, B. A., Nierenberg, C. A. J., Hoptman, M. J., Javitt, D. C., & Lim, K. O. (2003). MRI study of white matter diffusion anisotropy in schizophrenia. *Neuroreport*, *14*(16), 2025–2029. https://doi.org/10.1097/01.wnr.0000093290.85057

Arellano, G., Ottum, P. A., Reyes, L. I., Burgos, P. I., & Naves, R. (2015). Stage-specific role of interferon-gamma in experimental autoimmune encephalomyelitis and multiple sclerosis. *Frontiers in Immunology*, *6*(September), 1–9. https://doi.org/10.3389/fimmu.2015.00492

Arnett, H. A., Mason, J., Marino, M., Suzuki, K., Matsushima, G. K., & Ting, J. P. Y. (2001). TNFα promotes proliferation of oligodendrocyte progenitors and remyelination. *Nature Neuroscience*, *4*(11), 1116–1122. https://doi.org/10.1038/nn738

Baecher-Allan, C., Kaskow, B. J., & Weiner, H. L. (2018). Multiple sclerosis: Mechanisms and immunotherapy. *Neuron*, *97*(4), 742–768. https://doi.org/10.1016/j.neuron.2018.01.021

Barnett, M. H., & Prineas, J. W. (2004). Relapsing and remitting multiple sclerosis: Pathology of the newly forming lesion. *Annals of Neurology*, *55*(4), 458–468. https://doi.org/10.1002/ana.20016

Batoulis, H., Recks, M. S., Holland, F. O., Thomalla, F., Williams, R. O., & Kuerten, S. (2014). Blockade of tumour necrosis factor-α in experimental autoimmune encephalomyelitis reveals differential effects on the antigen-specific immune response and central nervous system histopathology. *Clinical and Experimental Immunology*, *175*(1), 41–48. https://doi.org/10.1111/cei.12209

Bernardo, A., Bianchi, D., Magnaghi, V., & Minghetti, L. (2009). Peroxisome proliferator-activated receptor-gamma agonists promote differentiation and antioxidant defenses of oligodendrocyte progenitor cells. *Journal of Neuropathology and Experimental Neurology*, *68*(7), 797–808. https://doi.org/10.1097/NEN.0b013e3181aba2c1

Bittner, S., Afzali, A. M., Wiendl, H., & Meuth, S. G. (2014). Myelin oligodendrocyte glycoprotein (MOG35-55) induced experimental autoimmune encephalomyellitis (EAE) in C57BL/6 mice. *Journal of Visualized Experiments*, (86), 3–7. https://doi.org/10.3791/51275

Bjartmar, C., Wujek, J. R., & Trapp, B. D. (2003). Axonal loss in the pathology of MS: Consequences for understanding the progressive phase of the disease. *Journal of the Neurological Sciences*, *206*, 165–171.

Bjelobaba, I., Begovic-Kupresanin, V., Pekovic, S., & Lavrnja, I. (2018). Animal models of multiple sclerosis: Focus on experimental autoimmune encephalomyelitis. *Journal of Neuroscience Research*, *96*(6), 1021–1042. https://doi.org/10.1002/jnr.24224

Boven, L. A., Van Meurs, M., Van Zwam, M., Wierenga-Wolf, A., Hintzen, R. Q., Boot, R. G., … Laman, J. D. (2006). Myelin-laden macrophages are anti-inflammatory, consistent with foam cells in multiple sclerosis. *Brain*, *129*(2), 517–526. https://doi.org/10.1093/brain/awh707

Brambilla, R., Ashbaugh, J. J., Magliozzi, R., Dellarole, A., Karmally, S., Szymkowski, D. E., & Bethea, J. R. (2011). Inhibition of soluble tumour necrosis factor is therapeutic in experimental autoimmune encephalomyelitis and promotes axon preservation and remyelination. *Brain*, *134*(9), 2736–2754. https://doi.org/10.1093/brain/awr199

Bustin, S. A., Benes, V., Garson, J. A., Hellemans, J., Huggett, J., Kubista, I., … Wittwer, C. T. (2009). The MIQE guidlines: Minimum information for publication of quantitative real-time PCR experiments. *Clinical Chemistry*, *55*(4), 611–622. https://doi.org/10.1373/clinchem.2008.112797

Calabresi, P. a. (2004). Diagnosis and management of multiple sclerosis. *American Family Physician*, *70*(10), 1935–1944. https://doi.org/10.1016/j.ejrad.2008.02.044

Cammer, W. (1999). The neurotoxicant, cuprizone, retards the differentiation of oligodendrocytes in vitro. *Journal of the Neurological Sciences*, *168*(2), 116–120. https://doi.org/10.1016/S0022-510X(99)00181-1

Caprariello, A. V, Rogers, J. A., Morgan, M. L., Hoghooghi, V., Plemel, J. R., Koebel, A., … Stys, P. K. (2018). Biochemically altered myelin triggers autoimmune demyelination. *Proceedings of the National Academy of Sciences*, *115*(22), 5528–5533. https://doi.org/10.1073/pnas.1721115115

Casella, G., Garzetti, L., Gatta, A. T., Finardi, A., Maiorino, C., Ruffini, F., … Furlan, R. (2016). IL4 induces IL6-producing M2 macrophages associated to inhibition of neuroinflammation in vitro and in vivo. *Journal of Neuroinflammation*, *13*(1), 1–10. https://doi.org/10.1186/s12974-016-0596-5

Compston, A., & Coles, A. (2008). Multiple sclerosis. *The Lancet*, *372*(9648), 1502–1517. https://doi.org/10.1016/S0140-6736(08)61620-7

Constantinescu, C. S., Farooqi, N., O'Brien, K., & Gran, B. (2011). Experimental autoimmune encephalomyelitis (EAE) as a model for multiple sclerosis (MS). *British Journal of Pharmacology*, *164*(4), 1079–1106. https://doi.org/10.1111/j.1476-5381.2011.01302.x

De Nuccio, C., Bernardo, A., De Simone, R., Mancuso, E., Magnaghi, V., Visentin, S., & Minghetti, L. (2011). Peroxisome proliferator-activated receptor γ agonists accelerate oligodendrocyte maturation and influence mitochondrial functions and oscillatory Ca2+ waves. *Journal of Neuropathology and Experimental Neurology*, *70*(10), 900–912. https://doi.org/10.1097/NEN.0b013e3182309ab1

Dendrou, C. A., Fugger, L., & Friese, M. A. (2015). Immunopathology of multiple sclerosis. *Nature Reviews Immunology*, *15*(9), 545–558. https://doi.org/10.1038/nri3871

Doring, A., Sloka, S., Lau, L., Mishra, M., van Minnen, J., Zhang, X., … Yong, V. W. (2015). Stimulation of monocytes, macrophages, and microglia by Amphotericin B and macrophage colony-stimulating factor promotes remyelination. *Journal of Neuroscience*, *35*(3), 1136–1148. https://doi.org/10.1523/JNEUROSCI.1797-14.2015

Eugster, H. Pietro, Frei, K., Bachmann, R., Bluethmann, H., Lassmann, H., & Fontana, A. (1999). Severity of symptoms and demyelination in MOG-induced EAE depends on TNFR1. *European Journal of Immunology*, *29*(2), 626–632.

Eugster, H. Pietro, Frei, K., Kopf, M., Lassmann, H., & Fontana, A. (1998). IL-6-deficient mice resist myelin oligodendrocyte glycoprotein-induced autoimmune encephalomyelitis. *European Journal of Immunology*, *28*(7), 2178–2187.

Feinstein, D. L., Galea, E., Gavrilyuk, V., Brosnan, C. F., Whitacre, C. C., Dumitrescu-Ozimek, L., … Heneka, M. T. (2002). Peroxisome proliferator-activated receptor-γ agonists prevent experimental autoimmune encephalomyelitis. *Annals of Neurology*, *51*(6), 694–702. https://doi.org/10.1002/ana.10206

Ferguson, B., Matyszak, M. K., Esiri, M. M., & Perry, V. H. (1997). Axonal damage in acute multiple sclerosis lesions. *Brain*, *120*(3), 393–399. https://doi.org/10.1093/brain/120.3.393

Flynn, S. W., Lang, D. J., Mackay, A. L., Goghari, V., Vavasour, I. M., Whittall, K. P., … Honer, W. G. (2003). Abnormalities of myelination in schizophrenia detected in vivo with MRI, and post-mortem with analysis of oligodendrocyte proteins. *Molecular Psychiatry*, *8*(9), 811–820. https://doi.org/10.1038/sj.mp.4001337

Foote, A. K., & Blakemore, W. F. (2005). Inflammation stimulates remyelination in areas of chronic demyelination. *Brain*, *128*(3), 528–539. https://doi.org/10.1093/brain/awh417

Franklin, R. J. M. (2002). Why does remyelination fail in multiple sclerosis? *Nature Reviews Neuroscience*, *3*(9), 705–714. https://doi.org/10.1038/nrn917

Franklin, R. J. M., & Ffrench-Constant, C. (2008). Remyelination in the CNS: From biology to therapy. *Nature Reviews Neuroscience*, *9*(11), 839–855. https://doi.org/10.1038/nrn2480

Frischer, J. M., Bramow, S., Dal-Bianco, A., Lucchinetti, C. F., Rauschka, H., Schmidbauer, M., … Lassmann, H. (2009). The relation between inflammation and neurodegeneration in multiple sclerosis brains. *Brain*, *132*(5), 1175–1189. https://doi.org/10.1093/brain/awp070

Furlan, R., Brambilla, E., Ruffini, F., Poliani, P. L., Bergami, A., Marconi, P. C., … Martino, G. (2001). Tranthecal delivery of IFN-gamma protects C57BL/6 mice from chronic-progressive experimental autoimmune encephalomyelitis by increasing apoptosis of central nervous system-infiltrating lymphocytes. *The Journal of Immunology*, *167*(3), 1821–1829. https://doi.org/10.4049/jimmunol.167.3.1821

Gay, F. W., Drye, T. J., Dick, G. W. A., & Esiri, M. M. (1997). The application of multifactorial cluster analysis in the staging of plaques in early multiple sclerosis: Identification and characterization of the primary demyelinating lesion. *Brain*, *120*(8), 1461–1483. https://doi.org/10.1093/brain/120.8.1461

Ghasemlou, N., Jeong, S. Y., Lacroix, S., & David, S. (2007). T cells contribute to lysophosphatidylcholine-induced macrophage activation and demyelination in the CNS. *Glia*, *55*, 294–302. https://doi.org/10.1002/glia

Gilmour, H., Ramage-Morin, P. L., & Wong, S. L. (2018). Multiple sclerosis: Prevalence and impact. *Health Reports*, *29*(1), 3–8. https://doi.org/no.82-003-X

Gold, R., Linington, C., & Lassmann, H. (2006). Understanding pathogenesis and therapy of multiple sclerosis via animal models: 70 Years of merits and culprits in experimental autoimmune encephalomyelitis research. *Brain*, *129*(8), 1953–1971. https://doi.org/10.1093/brain/awl075

Goldschmidt, T., Antel, J., König, F. B., Brück, W., & Kuhlmann, T. (2009). Remyelination capacity of the MS brain decreases with disease chronicity. *Neurology*, *72*(22), 1914–1921. https://doi.org/10.1212/WNL.0b013e3181a8260a

Green, L. K., Zareie, P., Templeton, N., Keyzers, R. A., Connor, B., & La Flamme, A. C. (2017). Enhanced disease reduction using clozapine, an atypical antipsychotic agent, and glatiramer acetate combination therapy in experimental autoimmune encephalomyelitis. *Multiple Sclerosis Journal*, 1–13. https://doi.org/10.1177/2055217317698724

Gregson, N. a. (1989). Lysolipids and membrane damage: Lysolecithin and its interaction with myelin. *Biochemical Society Transactions*, *17*(2), 280–283. https://doi.org/10.1042/bst0170280

Grommes, C., Karlo, J. C., Caprariello, A., Blankenship, D., Dechant, A., & Landreth, G. E. (2013). The PPARγ agonist pioglitazone crosses the blood-brain barrier and reduces tumor growth in a human xenograft model. *Cancer Chemotherapy and Pharmacology*, *71*(4), 929–936. https://doi.org/10.1007/s00280-013-2084-2

Hakak, Y., Walker, J. R., Li, C., Wong, W. H., Davis, K. L., Buxbaum, J. D., … Fienberg, A. A. (2001). Genome-wide expression analysis reveals dysregulation of myelination-related genes in chronic schizophrenia. *Proceedings of the National Academy of Sciences*, *98*(8), 4746–4751. https://doi.org/10.1073/pnas.081071198

Hall, S. M. (1972). The effect of injections of lysophosphatidyl choline into white matter of the adult mouse spinal cord. *Journal of Cell Science*, *10*, 535–546.

Hammarberg, H., Lidman, O., Lundberg, C., Eltayeb, S. Y., Gielen, a W., Muhallab, S., … Piehl, F. (2000). Neuroprotection by encephalomyelitis: rescue of mechanically injured neurons and neurotrophin production by CNS-infiltrating T and natural killer cells. *The Journal of Neuroscience*, *20*(14), 5283–5291. https://doi.org/10.1016/j.neuron.2012.03.026

Handel, A. E., Lincoln, M. R., & Ramagopalan, S. V. (2011). Of mice and men: Experimental autoimmune encephalitis and multiple sclerosis. *European Journal of Clinical Investigation*, *41*(11), 1254–1258. https://doi.org/10.1111/j.1365-2362.2011.02519.x

Hauben, E., Butovsky, O., Nevo, U., Yoles, E., Moalem, G., Agranov, E., … Schwartz, M. (2000). Passive or active immunization with myelin basoc protein promotes recovery from spinal cord contusion. *Journal of Neuroscience*, *20*(17), 6421–6430. Retrieved from http://www.jneurosci.org.pros.lib.unimi.it/content/20/17/6421.long

Höflich, K. M., Beyer, C., Clarner, T., Schmitz, C., Nyamoya, S., Kipp, M., & Hochstrasser, T. (2016). Acute axonal damage in three different murine models of multiple sclerosis: A comparative approach. *Brain Research*, *1650*, 125–133. https://doi.org/10.1016/j.brainres.2016.08.048

Jeffery, N. D., & Blakemore, W. F. (1995). Remyelination of mouse spinal cord axons demyelinated by local injection of lysolecithin. *Journal of Neurocytology*, *24*(10), 775–781. https://doi.org/10.1007/BF01191213

Jones, M. V., Nguyen, T. T., DeBoy, C. A., Griffin, J. W., Whartenby, K. A., Kerr, D. A., & Calabresi, P. A. (2008). Behavioral and pathological outcomes in MOG 35-55 experimental autoimmune encephalomyelitis. *Journal of Neuroimmunology*, *199*, 83–93. https://doi.org/10.1016/j.jneuroim.2008.05.013

Kahn, S. E., Cooper, M. E., & Del Prato, S. (2015). Pathophysiology and treatment of type 2 diabetes: Perspectives on the past, present and future. *Lancet*, *383*(9922), 1068–1083. Retrieved from http://www.ncbi.nlm.nih.gov/pubmed/24315620%0Ahttp://www.pubmedcentral.nih.gov/articlerender.fcgi?artid=PMC4226760

Kaiser, C. C., Shukla, D. K., Stebbins, G. T., Skias, D. D., Jeffery, D. R., Stefoski, D., … Feinstein, D. L. (2009). A pilot test of pioglitazone as an add-on in patients with relapsing remitting multiple sclerosis. *Journal of Neuroimmunology*, *211*(1–2), 124–130. https://doi.org/10.1016/j.jneuroim.2009.04.011

Kane, J., Honigfeld, G., Singer, J., & Meltzer, H. (1988). Clozapine for the treatment resistant schizophrenic. *Archives of General Psychiatry*, *45*, 789–796. https://doi.org/10.1001/archpsyc.1988.01800330013001

Keough, M. B., Jensen, S. K., & Yong, V. W. (2015). Experimental demyelination and remyelination of murine spinal cord by focal injection of lysolecithin. *Journal of Visualized Experiments*, (97), 1–8. https://doi.org/10.3791/52679

Khoury, S. J., Hancock, W. W., & Weiner, H. L. (1992). Oral tolerance to myelin basic protein and natural recovery from experimental autoimmune encephalomyelitis are associated with downregulation of inflammatory cytokines and differential upregulation of transforming growth factor B, interleukin 4, and prost. *Journal of Experimental Medicine*, *176*(November), 1355–1364. Retrieved from http://www.jneurosci.org/cgi/doi/10.1523/JNEUROSCI.1922-07.2007

Kirk, J., Plumb, J., Mirakhur, M., & McQuaid, S. (2003). Tight junctional abnormality in multiple sclerosis white matter affects all calibres of vessel and is associated with blood-brain barrier leakage and active demyelination. *Journal of Pathology*, *201*(2), 319–327. https://doi.org/10.1002/path.1434

Kıray, H., Lindsay, S. L., Hosseinzadeh, S., & Barnett, S. C. (2016). The multifaceted role of astrocytes in regulating myelination. *Experimental Neurology*, *283*, 541–549. https://doi.org/10.1016/j.expneurol.2016.03.009

Klotz, L., Diehl, L., Dani, I., Neumann, H., von Oppen, N., Dolf, A., … Knolle, P. (2007). Brain endothelial PPARγ controls inflammation-induced CD4+ T cell adhesion and transmigration in vitro. *Journal of Neuroimmunology*, *190*(1–2), 34–43. https://doi.org/10.1016/j.jneuroim.2007.07.017

Kotter, M. R., Li, W.-W., Zhao, C., & Franklin, R. J. M. (2006). Myelin impairs CNS remyelination by inhibiting oligodendrocyte precursor cell differentiation. *Journal of Neuroscience*, *26*(1), 328–332. https://doi.org/10.1523/JNEUROSCI.2615-05.2006

Kotter, M. R., Setzu, A., Sim, F. J., Van Rooijen, N., & Franklin, R. J. M. (2001). Macrophage depletion impairs oligodendrocyte remyelination following lysolecithin-induced demyelination. *Glia*, *35*(3), 204–212. https://doi.org/10.1002/glia.1085

Kotter, M. R., Zhao, C., Van Rooijen, N., & Franklin, R. J. M. (2005). Macrophage-depletion induced impairment of experimental CNS remyelination is associated with a reduced oligodendrocyte progenitor cell response and altered growth factor expression. *Neurobiology of Disease*, *18*(1), 166–175. https://doi.org/10.1016/j.nbd.2004.09.019

Kuhlmann, T., Ludwin, S., Prat, A., Antel, J., Brück, W., & Lassmann, H. (2017). An updated histological classification system for multiple sclerosis lesions. *Acta Neuropathologica*, *133*(1), 13–24. https://doi.org/10.1007/s00401-016-1653-y

Lalive, P. H., Paglinawan, R., Biollaz, G., Kappos, E. A., Leone, D. P., Malipiero, U., … Fontana, A. (2005). TGF-β-treated microglia induce oligodendrocyte precursor cell chemotaxis through the HGF-c-Met pathway. *European Journal of Immunology*, *35*(3), 727–737. https://doi.org/10.1002/eji.200425430

Lassmann, H., Brück, W., & Lucchinetti, C. F. (2007). The immunopathology of multiple sclerosis: An overview. *Brain Pathology*, *17*(2), 210–218. https://doi.org/10.1111/j.1750-3639.2007.00064.x

Lau, L. W., Keough, M. B., Haylock-Jacobs, S., Cua, R., Döring, A., Sloka, S., … Yong, V. W. (2012). Chondroitin sulfate proteoglycans in demyelinated lesions impair remyelination. *Annals of Neurology*, *72*(3), 419–432. https://doi.org/10.1002/ana.23599

Lévesque, S. A., Paré, A., Mailhot, B., Bellver-Landete, V., Kébir, H., Lécuyer, M.-A., … Lacroix, S. (2016). Myeloid cell transmigration across the CNS vasculature triggers IL-1β–driven neuroinflammation during autoimmune encephalomyelitis in mice. *The Journal of Experimental Medicine*, *213*(6), 929–949. https://doi.org/10.1084/jem.20151437

Liao, H.-W., Saver, J. L., Wu, Y.-L., Chen, T.-H., Lee, M., & Ovbiagele, B. (2017). Pioglitazone and cardiovascular outcomes in patients with insulin resistance, pre-diabetes and type 2 diabetes: A systematic review and meta-analysis. *BMJ Open*, *7*(1), e013927. https://doi.org/10.1136/bmjopen-2016-013927

Lin, C.-C., & Edelson, B. T. (2017). New insights in to the role of IL-1β in experimental autoimmune encephalomyelitis and multiple sclerosis. *The Journal of Immunology*, *198*(12), 4553–4560. https://doi.org/10.4049/jimmunol.1700263

Linker, R. A., Lee, D.-H., Demir, S., Wiese, S., Kruse, N., Siglienti, I., … Gold, R. (2010). Functional role of brain-derived neurotrophic factor in neuroprotective autoimmunity: Therapeutic implications in a model of multiple sclerosis. *Brain*, *133*(8), 2248–2263. https://doi.org/10.1093/brain/awq179

Loma, I., & Heyman, R. (2011). Multiple sclerosis: Pathogenesis and treatment. *Current Neuropharmacology*, *9*(3), 409–416. https://doi.org/10.2174/157015911796557911

Losseff, N. A., Wang, L., Lai, H. M., Yoo, D. S., Gawne-Cain, M. L., McDonald, W. I., … Thompson, A. J. (1996). Progressive cerebral atrophy in multiple sclerosis A serial MRI study. *Brain*, *119*(6), 2009–2019. https://doi.org/10.1093/brain/119.6.2009

Losseff, N. A., Webb, S. L., O'Riordan, J. I., Page, R., Wang, L., Barker, G. J., … Thompson, A. J. (1996). Spinal cord atrophy and disability in multiple sclerosis. A new reproducible and sensitive MRI method with potential to monitor disease progression. *Brain*, *119*(3), 701–708.

Madsen, P. M., Motti, D., Karmally, S., Szymkowski, D. E., Lambertsen, K. L., Bethea, J. R., & Brambilla, R. (2016). Oligodendroglial TNFR2 mediates membrane TNF-dependent repair in epxperimental autoimmune encephalomyelitis by promoting oligodendrocyte differentiation and remyelination. *The Journal of Neuroscience*, *36*(18), 5128–5143. https://doi.org/10.1523/JNEUROSCI.0211-16.2016

Maña, P., Fordham, S. A., Staykova, M. A., Correcha, M., Silva, D., Willenborg, D. O., & Liñares, D. (2009). Demyelination caused by the copper chelator cuprizone halts T cell mediated autoimmune neuroinflammation. *Journal of Neuroimmunology*, *210*(1–2), 13–21. https://doi.org/10.1016/j.jneuroim.2009.02.013

Mannara, F., Valente, T., Saura, J., Graus, F., Saiz, A., & Moreno, B. (2012). Passive experimental autoimmune encephalomyelitis in C57BL/6 with MOG: Evidence of involvement of B cells. *PLoS ONE*, *7*(12), 1–9. https://doi.org/10.1371/journal.pone.0052361

Markovic-Plese, S., Fukaura, H., Zhang, J., Al-Sabbagh, A., Southwood, S., Sette, A., … Hafler, D. A. (1995). T cell recognition of immunodominant and cryptic proteolipid protein epitopes in humans. *Journal of Immunology*, *155*(2), 982–992. Retrieved from http://www.jimmunol.org/content/155/2/982.abstract

Mason, J. L., Suzuki, K., Chaplin, D. D., & Matsushima, G. K. (2001). Interleukin-1beta promotes repair of the CNS. *Journal of Neuroscience*, *21*(18), 7046–7052. https://doi.org/21/18/7046 [pii]

Mendel, I., Katz, A., Kozak, N., Ben-Nun, A., & Revel, M. (1998). Interleukin-6 functions in autoimmune encephalomyelitis: A study in gene-targeted mice. *European Journal of Immunology*, *28*(5), 1727–1737.

Meriden, T. (2004). Progress with thiazolidinediones in the management of type 2 diabetes mellitus. *Clinical Therapeutics*, *26*(2), 177–190.

Miller, D. H., Chard, D. T., & Ciccarelli, O. (2012). Clinically isolated syndromes. *The Lancet Neurology*, *11*(2), 157–169. https://doi.org/10.1016/S1474-4422(11)70274-5

Miron, V. E., Boyd, A., Zhao, J. W., Yuen, T. J., Ruckh, J. M., Shadrach, J. L., … Ffrench-Constant, C. (2013). M2 microglia and macrophages drive oligodendrocyte differentiation during CNS remyelination. *Nature Neuroscience*, *16*(9), 1211–1218. https://doi.org/10.1038/nn.3469

Moalem, G., Gdalyahu, A., Shani, Y., Otten, U., Lazarovici, P., Cohen, I. R., & Schwartz, M. (2000). Production of neurotrophins by activated T cells: Implications for neuroprotective autoimmunity. *Journal of Autoimmunity*, *15*(3), 331–345. https://doi.org/10.1006/jaut.2000.0441

Moalem, G., Leibowitz-Amit, R., Yoles, E., Mor, F., Cohen, I. R., & Schwartz, M. (1999). Autoimmune T cells protect neurons from secondary degeneration after central nervous system axotomy. *Nature Medicine*, *5*(1), 49–55. https://doi.org/10.1038/4734

Montalban, X., Hauser, S. L., Kappos, L., Arnold, D. L., Bar-Or, A., Comi, G., … Wolinsky, J. S. (2017). Ocrelizumab versus placbeo in primary progressive multiple sclerosis. *New England Journal of Medicine*, *376*(3), 209–220. https://doi.org/10.1056/NEJMoa1606468

Naheed, M., & Green, B. (2001). Focus on clozapine. *Current Medical Research and Opinion*, *17*(3), 223–229. https://doi.org/10.1185/0300799039117069

Natrajan, M. S., Komori, M., Kosa, P., Johnson, K. R., Wu, T., Franklin, R. J. M., & Bielekova, B. (2015). Pioglitazone regulates myelin phagocytosis and multiple sclerosis monocytes. *Annals of Clinical and Translational Neurology*, *2*(12), 1071–1084. https://doi.org/10.1002/acn3.260

Negrotto, L., Farez, M. F., & Correale, J. (2016). Immunologic effects of metformin and pioglitazone treatment on metabolic syndrome and multiple sclerosis. *JAMA Neurology*, *73*(5), 520–528. https://doi.org/10.1001/jamaneurol.2015.4807

O'Sullivan, D., Green, L., Stone, S., Zareie, P., Kharkrang, M., Fong, D., … La Flamme, A. C. (2014). Treatment with the antipsychotic agent, risperidone, reduces disease severity in experimental autoimmune encephalomyelitis. *PLoS ONE*, *9*(8), 1–12. https://doi.org/10.1371/journal.pone.0104430

Olsson, T. (1995). Critical influences of the cytokine orchestration on the outcome of myelin antigen-specific T-cell autoimmunity in experimental autoimmune encephalomyelitis and multiple sclerosis. *Immunological Reviews*, *144*(1), 245–268. https://doi.org/10.1111/j.1600-065X.1995.tb00072.x

Ousman, S. S., & David, S. (2000). Lysophosphatidylcholine induces rapid recruitment and activation of macrophages in the adult mouse spinal cord. *Glia*, *30*(1), 92–104. Retrieved from http://onlinelibrary.wiley.com/store/10.1002/(SICI)1098-1136(200003)30:1%3C92::AID-GLIA10%3E3.0.CO;2-W/asset/10_ftp.pdf?v=1&t=ieebtwfk&s=07f8cd14b1d3efc8aa8d31c5e8858d4f77d32cb1&systemMessage=Wiley+Online+Library+and+related+systems+will+have+3+hours+of+d

Owen, M. J., Sawa, A., & Mortensen, P. B. (2016). Schizophrenia. *The Lancet*, *388*, 86–97. https://doi.org/10.1016/S0140-6736(15)01121-6

Papadopoulos, N. M., Cevallos, W., & Hess, W. C. (1960). Determination of phospholipids in spinal fluid and brain. *Archives of Neurology*, *3*, 85–90.

Patel, K. R., Cherian, J., Gohil, K., & Atkinson, D. (2014). Schizophrenia: overview and treatment options. *P & T: A Peer-Reviewed Journal for Formulary Management*, *39*(9), 638–645.

Pershadsingh, H. A., Heneka, M. T., Saini, R., Amin, N. M., Broeske, D. J., & Feinstein, D. L. (2004). Effect of pioglitazone treatment in a patient with secondary multiple sclerosis. *Journal of Neuroinflammation*, *1*, 1–4. https://doi.org/10.1186/1742-2094-1-3

Plemel, J. R., Michaels, N. J., Weishaupt, N., Caprariello, A. V., Keough, M. B., Rogers, J. A., … Yong, V. W. (2018). Mechanisms of lysophosphatidylcholine-induced demyelination: A primary lipid disrupting myelinopathy. *Glia*, *66*(2), 327–347. https://doi.org/10.1002/glia.23245

Ponomarev, E. D., Maresz, K., Tan, Y., & Dittel, B. N. (2007). CNS-derived interleukin-4 is essential for the regulation of autoimmune inflammation and induces a state of alternative activation in microglial cells. *Journal of Neuroscience*, *27*(40), 10714–10721. https://doi.org/10.1523/JNEUROSCI.1922-07.2007

Rawji, K. S., Mishra, M. K., & Yong, V. W. (2016). Regenerative capacity of macrophages for remyelination. *Frontiers in Cell and Developmental Biology*, *4*(May), 1–8. https://doi.org/10.3389/fcell.2016.00047

Rawji, K. S., & Yong, V. W. (2013). The benefits and detriments of macrophages/microglia in models of multiple sclerosis. *Clinical and Developmental Immunology*, *2013*(2013), 1–13.

Reich, D. S., Lucchinetti, C. F., & Calabresi, P. A. (2018). Multiple Sclerosis. *New England Journal of Medicine*, *378*(2), 169–180. https://doi.org/10.1056/NEJMra1401483

Renno, T., Krakowski, M., Piccirillo, C., Lin, J., & Owens, T. (1995). TNF-alpha expression by resident microglia and infiltrating leukocytes in the central nervous system of mice with experimental allergic encephalomyelitis. Regulation by Th1 cytokines. *Journal of Immunology*, *154*, 944–953. https://doi.org/10.4049/jimmunol.164.4.2070

Renno, T., Krawkoski, M., Piccirillo, C., Lin, J., & Owens, T. (1995). TNF-alpha expression by resident microglia and infiltrating leukocytes in the central nervous system with experimental allergic encephalomyelitis. Regulation by Th1 cytokines. *Journal of Immunology*, *154*, 944–953. https://doi.org/10.4049/jimmunol.164.4.2070

Rüther, B. J., Scheld, M., Dreymueller, D., Clarner, T., Kress, E., Brandenburg, L. O., … Kipp, M. (2017). Combination of cuprizone and experimental autoimmune encephalomyelitis to study inflammatory brain lesion formation and progression. *Glia*, *65*(12), 1900–1913. https://doi.org/10.1002/glia.23202

Samoilova, E. B., Horton, J. L., Hilliard, B., Liu, T.-S. T., & Chen, Y. (1998). IL-6-deficient mice are resistant to experimental autoimmune encephalomyelitis: Roles of IL-6 in the activation and differentiation of autoreactive T cells. *Journal of Immunology*, *161*, 6480–6486.

Scheld, M., Ruther, B. J., Grosse-Veldmann, R., Ohl, K., Tenbrock, K., Dreymuller, D., … Kipp, M. (2016). Neurodegeneration triggers peripheral immune cell recruitment into the forebrain. *Journal of Neuroscience*, *36*(4), 1410–1415. https://doi.org/10.1523/JNEUROSCI.2456-15.2016

Schernthaner, G., Matthews, D. R., Charbonnel, B., Hanefeld, M., & Brunetti, P. (2004). Efficacy and safety of pioglitazone versus metformin in patients with type 2 diabetes mellitus: A double-blind, randomized trial. *Journal of Clinical Endocrinology and Metabolism*, *89*(12), 6068–6076. https://doi.org/10.1210/jc.2003-030861

Schmidt, S., Moric, E., Schmidt, M., Sastre, M., Feinstein, D. L., & Heneka, M. T. (2004). Anti-inflammatory and antiproliferative actions of PPAR-gamma agonists on T lymphocytes derived from MS patients. *Journal of Leukocyte Biology*, *75*(3), 478–485. https://doi.org/10.1189/jlb.0803402

Schultz, V., van der Meer, F., Wrzos, C., Scheidt, U., Bahn, E., Stadelmann, C., … Junker, A. (2017). Acutely damaged axons are remyelinated in multiple sclerosis and experimental models of demyelination. *Glia*, *65*(8), 1350–1360. https://doi.org/10.1002/glia.23167

Seeman, P. (2014). Clozapine, a fast-off-D2 antipsychotic. *ACS Chemical Neuroscience*, *5*(1), 24–29. https://doi.org/10.1021/cn400189s

Smith, L. R., Kono, D. H., & Theofilopoulos, A. N. (1991). Prevention and treatment of chronic relapsing experimental autoimmune encephalomyelitis by transforming growth factor-beta 1. *The Journal of Immunology*, *146*, 3012–3017.

Sonar, S. A., Shaikh, S., Joshi, N., Atre, A. N., & Lal, G. (2017). IFN-γ 3 promotes transendothelial migration of CD4 + T cells across the blood-brain barrier. *Immunology and Cell Biology*, *95*(9), 843–853. https://doi.org/10.1038/icb.2017.56

Sriram, S., & Steiner, I. (2005). Experimental allergic encephalomyelitis: A misleading model of multiple sclerosis. *Annals of Neurology*, *58*(6), 939–945. https://doi.org/10.1002/ana.20743

Steiner, J., Martins-de-Souza, D., Schiltz, K., Sarnyai, Z., Westphal, S., Isermann, B., … Keilhoff, G. (2014). Clozapine promotes glycolysis and myelin lipid synthesis in cultured oligodendrocytes. *Frontiers in Cellular Neuroscience*, *8*(November), 1–11. https://doi.org/10.3389/fncel.2014.00384

Storch, M. K., Piddlesden, S., Haltia, M., Iivanainen, M., Morgan, P., & Lassmann, H. (1998). Multiple sclerosis: in situ evidence for antibody-and complement-mediated demyelination. *Annals of Neurology*, *43*(4), 465–471.

Storer, P. D., Xu, J., Chavis, J., & Drew, P. D. (2005). Peroxisome proliferator-activated receptor-gamma agonists inhibit the activation of microglia and astrocytes: Implications for multiple sclerosis. *Journal of Neuroimmunology*, *161*, 113–122. https://doi.org/10.1016/j.jneuroim.2004.12.015

Stroup, T. S., Gerhard, T., Crystal, S., Huang, C., & Olfson, M. (2016). Comparative effectiveness of clozapine and standard antipsychotic treatment in adults with schizophrenia. *American Journal of Psychiatry*, *173*(2), 166–173. https://doi.org/10.1176/appi.ajp.2015.15030332

Tejedor, L. S., Wostradowski, T., Gingele, S., Skripuletz, T., Gudi, V., & Stangel, M. (2017). The effect of stereotactic injections on demyelination and remyelination: A study in the cuprizone model. *Journal of Molecular Neuroscience*, *61*(4), 479–488. https://doi.org/10.1007/s12031-017-0888-y

The Lenercept Multiple Sclerosis Study Group. (1999). TNF neutralization in MS: Results of a randomized, placebo-controlled multicenter study. *Neurology*, *53*, 457–465. https://doi.org/10.1212/WNL.53.3.457

Torkildsen, Brunborg, L. A., Myhr, K. M., & Bø, L. (2008). The cuprizone model for demyelination. *Acta Neurologica Scandinavica*, *117*(SUPPL. 188), 72–76. https://doi.org/10.1111/j.1600-0404.2008.01036.x

Trapp, B. D., Peterson, J., Ransohoff, R. M., Rudick, R., Mörk, S., & Bö, L. (1998). Axonal transections in the lesions of multiple sclerosis. *New England Journal of Medicine*, *338*(5), 278–285. https://doi.org/10.1056/NEJM199801293380502

Triarhou, L. C., & Herndon, R. M. (1985). Effect of macrophage inactivation on the neuropathology of lysolecithin-induced demyelination. *British Journal of Experimental Pathology*, *66*(3), 293–301. Retrieved from http://www.pubmedcentral.nih.gov/articlerender.fcgi?artid=2041059&tool=pmcentrez&rendertype=abstract

van Zwam, M., Huizinga, R., Heijman, N., van Meurs, M., Wierenga-Wolf, A. F., Meleif, M.-J., … Laman, J. D. (2009). Surgical excision of CNS-draining lymph nodes reduces relapse severity in chronic-relapsing experimental autoimmune encephalomyelitis. *The Journal of Pathology*, *217*, 543–551. https://doi.org/10.1002/path

VonDran, M. W., Singh, H., Honeywell, J. Z., & Dreyfus, Ch. F. (2011). Levels of BDNF impact oligodendrocyte lineage cells following a cuprizone lesion. *Journal of Neuroscience*, *31*(40), 14182–14190. https://doi.org/10.1007/s10439-011-0452-9.Engineering

Webster, G., & Alpern, R. (1964). Studies on the acylation of lysolecithin by rat brains. *Biochemical Journal*, *90*(35), 35–42.

Wolpe, S. D., Sherry, B., Juers, D., Davatelis, G., Yurt, R. W., & Cerami, A. (1989). Identification and characterization of macrophage inflammatory protein 2. *Proceedings of the National Academy of Sciences of the United States of America*, *86*(2), 612–616. https://doi.org/10.1073/pnas.86.2.612

Xu, H., Yang, H.-J., & Li, X.-M. (2014). Differential effects of antipsychotics on the development of rat oligodendrocyte precursor cells exposed to cuprizone. *European Archives of Psychiatry and Clinical Neuroscience*, *264*(2), 121–129. https://doi.org/10.1007/s00406-013-0414-3

Xu, H., Yang, H., Mcconomy, B., Browning, R., & Li, X. (2010). Behavioral and neurobiological changes in C57BL / 6 mouse exposed to cuprizone : effects of antipsychotics CHEMICALS AND REAGENTS. *Frontiers in Behavioral Neuroscience*, *4*(March), 1–10. https://doi.org/10.3389/fnbeh.2010.00008

Zhang, B. J., Markovic-plese, S., Lacet, B., Raus, J., Weiner, H. L., & Hailer, D. a. (1994). Increased frequency of interleukin 2-responsive T cells specific for myelin basic protein and proteolipid protein in peripheral blood and cerebrospinal fluid of patients with multiple sclerosis. *Journal of Experimental Medicine*, *179*(March), 973–984.